

Triple the gamma – A unifying shrinkage prior for variance and variable selection in sparse state space and TVP models

Annalisa Cadonna ¹, Sylvia Frühwirth-Schnatter ^{1,*} and Peter Knaus ¹

¹ WU, Vienna University of Economics and Business

* Correspondence: sfruehwi@wu.ac.at

Received: date; Accepted: date; Published: date

Abstract: Time-varying parameter (TVP) models are very flexible in capturing gradual changes in the effect of a predictor on the outcome variable. However, in particular when the number of predictors is large, there is a known risk of overfitting and poor predictive performance, since the effect of some predictors is constant over time. We propose a prior for variance shrinkage in TVP models, called triple gamma. The triple gamma prior encompasses a number of priors that have been suggested previously, such as the Bayesian lasso, the double gamma prior and the Horseshoe prior. We present the desirable properties of such prior and its relationship to Bayesian Model Averaging for variance selection. The features of the triple gamma prior are then illustrated in the context of time varying parameter vector autoregressive models, both for simulated dataset and for a series of macroeconomics variables in the Euro Area.

Keywords: TVP models; triple gamma; Bayesian Model Averaging.

1. Introduction

Model selection in a high-dimensional setting is a common challenge in statistical and econometric inference. The introduction of Bayesian model averaging (BMA) techniques in the statistical literature [1–3] has led to many interesting applications, see, among others, [4–7] for early references in econometrics.

Predictor selection for possibly very high-dimensional regression problems through shrinkage priors is an attractive alternative to BMA which relies on discrete mixture priors, see Bhadra *et al.* [8] for an excellent review. There is a vast and growing literature on shrinkage priors for regression problems that focuses on the following aspects. First, how to choose sensible priors for high-dimensional model selection problems in a Bayesian framework, second, how to design efficient algorithms to cope with the associated computational challenges and third, to investigate, both from a theoretical and a practical viewpoint, how such priors perform in high-dimensional problems.

A striking duality exists in this very active area between Bayesian and traditional approaches. For many shrinkage priors, the mode of the posterior distribution obtained in a Bayesian analysis can be regarded as a point estimate from a regularization approach, see Fahrmeir *et al.* [9] and Polson and Scott [10]. One such example is the popular Lasso [11] which is equivalent to a double-exponential shrinkage prior in a Bayesian context [12]. However, the two approaches differ when it comes to selecting penalty parameters that impact the sparsity of the solution. One advantage of the Bayesian framework in this context is that the penalty parameters are considered to be unknown hyperparameters which can be learned from the data. Such “global-local” shrinkage priors [13] adjust to the overall degree of sparsity that is required in a specific application through a global shrinkage parameter and separates signal from noise through local, individual shrinkage parameters.

While predictor selection through shrinkage priors in regression models is addressed in a vast literature, the use of shrinkage priors for more general econometric models for time series analysis, such as state space models and time-varying parameter (TVP) models is, in comparison, less well-studied. Sparsity in the context of such models refers to the presence of a few large variances among many (nearly) zero variances in the latent state processes that drive the observed time series data. A common goal in this setting is to recover a few dynamic states, driven by such a state space model, among many (nearly) constant coefficients. As shown by Frühwirth-Schnatter and Wagner [14], this variance selection problem can be cast into a variable selection problem in the non-centered parametrization of a state space model. Once this link has been established, shrinkage priors that are known to perform well in high-dimensional regression problems can be applied to variance selection in state space models, as demonstrated for the Lasso [15] and the normal-gamma [16,17].

Despite this already existing variety, we introduce a new shrinkage prior for variance selection in sparse state space and TVP models in the present paper, called triple gamma prior as it has a representation involving three gamma distributions. This prior can be related to various shrinkage priors that were found to be useful for high-dimensional regression problems such as the generalized beta mixture prior [18] and contains the popular Horseshoe prior [19,20] as a special case. Furthermore, the half- t and the half Cauchy [21,22], suggested as robust alternatives to the inverse gamma distribution for variance parameters in hierarchical models, as well as the Lasso and the double gamma, are special cases of the triple gamma. In this context, the triple gamma can also be regarded as an extension of the scaled beta2 distribution [23].

Among Bayesian shrinkage priors, usually a clear distinction is made between two-group mixture or spike-and-slab priors and continuous shrinkage priors, of which the triple gamma is a special case. An important contribution of the present paper is to show that the triple gamma provides a bridge between these two approaches and has the following property which is favourable both in sparse and dense situations. One of the hyperparameters allows high concentration over the region in the shrinkage profile that is relevant for shrinking noise, while the other hyperparameter allows high concentration over the region that prevents overshrinking of signals. This leads to a behaviour of the triple gamma prior that very much resembles Bayesian model averaging based on discrete spike-and-slab priors, with a strong prior concentration at the corner solutions where some of the variances are nearly close to zero. While this is reminiscent of the Horseshoe prior, the shrinkage profile induced by the triple gamma is more flexible than that of a Horseshoe. Thanks to the estimation of the hyperparameters, it is not constrained to be symmetric around one half, enabling adaption to varying degrees of sparsity in the data.

The triple gamma prior also scores well from a computational perspective. While exploring the full posterior distribution for spike-and-slab priors leads to computational challenges due to the combinatorial complexity of the model space, Bayesian inference based on Markov chain Monte Carlo (MCMC) methods is straightforward for continuous shrinkage priors, exploiting their Gaussian-scale mixture representation [17,24]. An extension of these schemes to the triple gamma prior is fairly straightforward.

We will study the empirical performance of the triple gamma for a challenging setting in econometric time series analysis, namely for time-varying parameter vector autoregressive models with stochastic volatility (TVP-VAR-SV models). Since the influential paper of Primiceri [25] (see Del Negro and Primiceri [26] for a corrigendum), this model has become a benchmark for analyzing relationships between macroeconomic variables that evolve over time, see Nakajima [27], Koop and Korobilis [28], Eisenstat *et al.* [29], Chan and Eisenstat [30], Feldkircher *et al.* [31] and Carriero *et al.* [32], among many others. Due to the high dimensionality of the time-varying parameters, even for moderately sized systems, shrinkage priors such as the triple gamma prior are instrumental for efficient inference.

The rest of the paper is organized as follows. In Section 2, we define the triple gamma prior and discuss some of its properties. The close relationship between the triple gamma and spike-and-slab priors

applied in a BMA context is investigated in Section 3.2. Section 4 introduced an efficient MCMC scheme and Section 5 provides applications to TVP-VAR-SV models. Section 6 concludes the paper.

2. The triple gamma as a prior for variance parameters

2.1. Motivation and definition

Let us recall the state space form of a TVP model. For $t = 1, \dots, T$, we have that

$$\begin{aligned} \beta_t &= \beta_{t-1} + \mathbf{w}_t, & \mathbf{w}_t &\sim \mathcal{N}_d(\mathbf{0}, \mathbf{Q}), \\ y_t &= \mathbf{x}_t \beta_t + \varepsilon_t, & \varepsilon_t &\sim \mathcal{N}(0, \sigma_t^2), \end{aligned} \quad (1)$$

where $\mathbf{Q} = \text{Diag}(\theta_1, \dots, \theta_d)$, y_t is a univariate response variable, $\mathbf{x}_t = (x_{t1}, \dots, x_{td})$ is a d -dimensional row vector containing the regressors at time t , with x_{t1} corresponding to the intercept, and the initial value follows a normal distribution, $\beta_0 \sim \mathcal{N}_d(\beta, \mathbf{Q})$, with initial mean $\beta = (\beta_1, \dots, \beta_d)^\top$. Model (1) can be rewritten equivalently in the non-centered parametrization introduced in Frühwirth-Schnatter and Wagner [14] as

$$\begin{aligned} \tilde{\beta}_t &= \tilde{\beta}_{t-1} + \tilde{\mathbf{w}}_t, & \tilde{\mathbf{w}}_t &\sim \mathcal{N}_d(\mathbf{0}, \mathbf{I}_d), \\ y_t &= \mathbf{x}_t \beta + \mathbf{x}_t \text{Diag}(\sqrt{\theta_1}, \dots, \sqrt{\theta_d}) \tilde{\beta}_t + \varepsilon_t, & \varepsilon_t &\sim \mathcal{N}(0, \sigma_t^2), \end{aligned} \quad (2)$$

with $\tilde{\beta}_0 \sim \mathcal{N}_d(\mathbf{0}, \mathbf{I}_d)$, where \mathbf{I}_d is the d -dimensional identity matrix. The error variance in the observation equation is either homoscedastic ($\sigma_t^2 \equiv \sigma^2$ for all $t = 1, \dots, T$) or follows a stochastic volatility (SV) specification [33], where the log volatility $h_t = \log \sigma_t^2$ follows an AR(1) process. Specifically,

$$h_t | h_{t-1}, \mu, \phi, \sigma_\eta^2 \sim \mathcal{N}(\mu + \phi(h_{t-1} - \mu), \sigma_\eta^2). \quad (3)$$

To motivate the triple gamma prior, let us recall that, in TVP models, shrinkage priors are placed on each scale parameter $\sqrt{\theta_j}$, $j = 1, \dots, d$, in order to shrink dynamic coefficients to static ones, hence avoiding overfitting. One of such priors is the double gamma prior, employed recently by [17] for shrinkage of variances. The double gamma prior can be expressed as a scale-mixture of gamma distributions, with the following hierarchical representation:

$$\theta_j | \zeta_j^2 \sim \mathcal{G}\left(\frac{1}{2}, \frac{1}{2\zeta_j^2}\right), \quad \zeta_j^2 | a^\zeta, \kappa_B^2 \sim \mathcal{G}\left(a^\zeta, \frac{a^\zeta \kappa_B^2}{2}\right). \quad (4)$$

In the double gamma prior, each innovation variance θ_j is mixed over its own ζ_j^2 , each of which has an independent gamma distribution, with a common hyperparameter κ_B^2 . Moreover, the parameters ζ_j^2 play the role of local (component specific) shrinkage parameters, while the parameter κ_B^2 is a (common) global shrinkage parameter.

We propose an extension of the double gamma prior to a triple gamma prior, where another layer is added to the hierarchy:

$$\theta_j | \zeta_j^2 \sim \mathcal{G}\left(\frac{1}{2}, \frac{1}{2\zeta_j^2}\right), \quad \zeta_j^2 | a^\zeta, \kappa_j^2 \sim \mathcal{G}\left(a^\zeta, \frac{a^\zeta \kappa_j^2}{2}\right), \quad \kappa_j^2 | c^\zeta, \kappa_B^2 \sim \mathcal{G}\left(c^\zeta, \frac{c^\zeta}{\kappa_B^2}\right). \quad (5)$$

The main difference with the double gamma prior is that the ξ_j are not identically distributed, but each one depends on its component specific parameter κ_j^2 . Prior (5) contains many well-known shrinkage priors as a special case, as will be discussed in Section 2.3.

To make the shrinkage behaviour of the triple gamma prior more apparent, we will work with representations that involve the scale parameter $\sqrt{\theta_j}$, rather than the variance θ_j , using the fact that $\theta_j|\xi_j^2 \sim \xi_j^2\chi_1^2$ follows a re-scaled χ_1^2 -distribution. If we consider both the positive and the negative root of θ_j , then we obtain

$$\sqrt{\theta_j}|\xi_j^2 \sim \mathcal{N}\left(0, \xi_j^2\right), \quad \xi_j^2|a^\xi, \kappa_j^2 \sim \mathcal{G}\left(a^\xi, \frac{a^\xi \kappa_j^2}{2}\right), \quad \kappa_j^2|c^\xi, \kappa_B^2 \sim \mathcal{G}\left(c^\xi, \frac{c^\xi}{\kappa_B^2}\right). \quad (6)$$

Hence, prior (5) corresponds to $\sqrt{\theta_j}$ following the so-called normal-gamma-gamma prior consider by Griffin and Brown [16] in the context of defining hierarchical shrinkage priors for regression models.

To allow shrinkage of dynamic coefficients toward fixed, but significant ones, we extend Bitto and Frühwirth-Schnatter [17] further by assuming such a normal-gamma-gamma prior on the fixed parameter β_1, \dots, β_d :

$$\beta_j|\tau_j^2 \sim \mathcal{N}\left(0, \tau_j^2\right), \quad \tau_j^2|a^\tau, \lambda_j^2 \sim \mathcal{G}\left(a^\tau, \frac{a^\tau \lambda_j^2}{2}\right), \quad \lambda_j^2|c^\tau, \lambda_B^2 \sim \mathcal{G}\left(c^\tau, \frac{c^\tau}{\lambda_B^2}\right). \quad (7)$$

In Section 2.4, we will discuss hierarchical versions of both priors, by putting a hyperprior on the parameters $\kappa_B^2, \lambda_B^2, a^\xi, a^\tau, c^\xi$, and c^τ .

2.2. Properties of the triple gamma prior

It will be shown in Theorem 1 that the triple gamma prior is a global-local shrinkage prior in the sense of Polson and Scott [10] where the local shrinkage parameters arise from the F ($2a^\xi, 2c^\xi$) distribution. This representation allows to relate the triple gamma to the well-known Horseshoe prior, see Section 2.3. Furthermore, a closed form of the marginal shrinkage prior $p(\sqrt{\theta_j}|\phi^\xi, a^\xi, c^\xi)$ is given in Theorem 1, which is proven in Appendix A.

Theorem 1. For the triple gamma prior defined in (5), with $a^\xi > 0$ and $c^\xi > 0$, the following holds:

(a) It has following representation as a local-global shrinkage prior:

$$\sqrt{\theta_j}|\psi_j^2, \kappa_B^2 \sim \mathcal{N}\left(0, \frac{2}{\kappa_B^2} \psi_j^2\right), \quad \psi_j^2|a^\xi, c^\xi \sim \text{F}\left(2a^\xi, 2c^\xi\right). \quad (8)$$

(b) The marginal prior $p(\sqrt{\theta_j}|\phi^\xi, a^\xi, c^\xi)$ takes the following form with $\phi^\xi = \frac{2c^\xi}{\kappa_B^2 a^\xi}$,

$$p(\sqrt{\theta_j}|\phi^\xi, a^\xi, c^\xi) = \frac{\Gamma(c^\xi + \frac{1}{2})}{\sqrt{2\pi\phi^\xi} B(a^\xi, c^\xi)} U\left(c^\xi + \frac{1}{2}, \frac{3}{2} - a^\xi, \frac{\theta_j}{2\phi^\xi}\right), \quad (9)$$

where $U(a, b, z)$ is the confluent hyper-geometric function of the second kind:

$$U(a, b, z) = \frac{1}{\Gamma(a)} \int_0^\infty e^{-zt} t^{a-1} (1+t)^{b-a-1} dt.$$

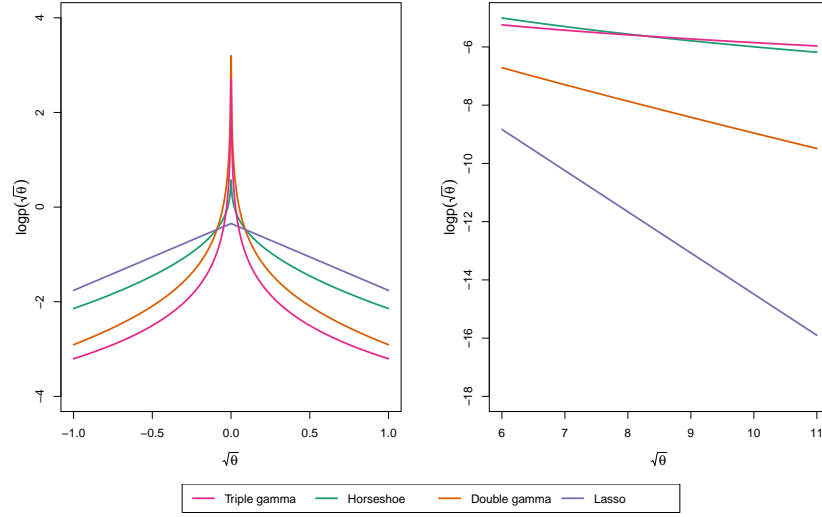


Figure 1. Marginal prior distribution of $\sqrt{\theta_j}$ under the triple gamma prior with $a^{\xi} = c^{\xi} = 0.1$ with $\kappa_B^2 = 2$, in comparison to the Horseshoe prior with $\phi^{\xi} = 1$, the double gamma prior with $a^{\xi} = 0.1$ and $\kappa_B^2 = 2$ and the Lasso prior with $\kappa_B^2 = 2$. (a) On the left, spike of the marginal prior distributions. (b) On the right, tail of the marginal prior distributions.

In Figure 1 we can see the marginal prior distribution of $\sqrt{\theta_j}$ under the triple gamma prior $a^{\xi} = c^{\xi} = 0.1$ and under other well-known shrinkage priors which are special cases of the triple gamma, see Table 1. Using Bitto and Frühwirth-Schnatter [17, Footnote 3], Theorem 1 also allows to give a closed form for the prior $p(\theta_j | \phi^{\xi}, a^{\xi}, c^{\xi}) = p(\sqrt{\theta_j} | \phi^{\xi}, a^{\xi}, c^{\xi}) / \sqrt{\theta_j}$.

Global-local shrinkage priors are typically compared in terms of the concentration around the origin and the tail behaviour. For the triple gamma prior $p(\sqrt{\theta_j} | \phi^{\xi}, a^{\xi}, c^{\xi})$, the two shape parameters a^{ξ} and c^{ξ} play a crucial role in this respect, see Theorem 2 which is proven in Appendix A.

Theorem 2. *The triple gamma prior (9) satisfies the following:*

(a) For $0 < a^{\xi} < 0.5$ and small values of $\sqrt{\theta_j}$,

$$p(\sqrt{\theta_j} | \phi^{\xi}, a^{\xi}, c^{\xi}) = \frac{\Gamma(\frac{1}{2} - a^{\xi})}{\sqrt{\pi}(2\phi^{\xi})^{a^{\xi}} B(a^{\xi}, c^{\xi})} \left(\frac{1}{\sqrt{\theta_j}} \right)^{1-2a^{\xi}} + O(1).$$

(b) For $a^{\xi} = 0.5$ and small values of $\sqrt{\theta_j}$,

$$p(\sqrt{\theta_j} | \phi^{\xi}, a^{\xi}, c^{\xi}) = \frac{1}{\sqrt{2\pi\phi^{\xi}} B(a^{\xi}, c^{\xi})} \left(-\log \theta_j + \log(2\phi^{\xi}) - \psi(c^{\xi} + \frac{1}{2}) \right) + O(|\theta_j \log \theta_j|),$$

where $\psi(\cdot)$ is the digamma function.

(c) For $a^{\xi} > 0.5$,

$$\lim_{\sqrt{\theta_j} \rightarrow 0} p(\sqrt{\theta_j} | \phi^{\xi}, a^{\xi}, c^{\xi}) = \frac{\Gamma(c^{\xi} + \frac{1}{2}) \Gamma(a^{\xi} - \frac{1}{2})}{\sqrt{2\pi} \phi^{\xi} B(a^{\xi}, c^{\xi}) \Gamma(a^{\xi} + c^{\xi})}.$$

(d) As $\sqrt{\theta_j} \rightarrow \infty$,

$$p(\sqrt{\theta_j} | \phi^{\xi}, a^{\xi}, c^{\xi}) = \frac{\Gamma(c^{\xi} + \frac{1}{2}) (2\phi^{\xi})^{c^{\xi}}}{\sqrt{\pi} B(a^{\xi}, c^{\xi})} \left(\frac{1}{\sqrt{\theta_j}} \right)^{2c^{\xi}+1} \left[1 + O\left(\frac{1}{\theta_j} \right) \right].$$

From Theorem 2, Part (a) and (b), we find that the triple gamma prior $p(\sqrt{\theta_j} | \phi^{\xi}, a^{\xi}, c^{\xi})$ has a pole at the origin, if $a^{\xi} \leq 0.5$. According to Part (a), the pole is more pronounced, the closer a^{ξ} gets to 0. For $a^{\xi} > 0.5$, we find from Part (c) that $p(\sqrt{\theta_j} | \phi^{\xi}, a^{\xi}, c^{\xi})$ is bounded at zero by a positive upper bound which is finite, as long as $0 < c^{\xi} < \infty$. Part (d) shows that the triple gamma prior $p(\sqrt{\theta_j} | \phi^{\xi}, a^{\xi}, c^{\xi})$ has polynomial tails, with the shape parameter c^{ξ} controlling the tail index. Prior moments $E((\sqrt{\theta_j})^k | \phi^{\xi}, a^{\xi}, c^{\xi})$ exist up to $k < 2c^{\xi}$. Hence, the triple gamma prior has no finite moments for $c^{\xi} < 1/2$.

Finally, additional useful representations of the triple gamma prior as a global-local shrinkage prior are summarized in Lemma 1 which is proven in Appendix A. Representations (a) shows that the triple gamma is an extension of the double gamma prior where the Gaussian prior $\sqrt{\theta_j} | \xi_j^2 \sim \mathcal{N}(0, \xi_j^2)$ is substituted by a heavier-tailed Student- t prior, making the prior more robust to large values of $\sqrt{\theta_j}$. Representation (b) and (c) will be useful for MCMC inference in Section 4. Representations (c) and (d) show that for a triple gamma prior with finite a^{ξ} and c^{ξ} , ϕ^{ξ} acts as a global shrinkage parameter, in addition to $2/\kappa_B^2$.

Lemma 1. For $a^{\xi} > 0$ and $c^{\xi} > 0$, the triple gamma prior (5) has the following alternative representations:

$$(a) \quad \sqrt{\theta_j} | \check{\xi}_j^2, c^{\xi}, \kappa_B^2 \sim t_{2c^{\xi}} \left(0, \frac{2}{\kappa_B^2} \check{\xi}_j^2 \right), \quad \check{\xi}_j^2 | a^{\xi} \sim \mathcal{G}(a^{\xi}, a^{\xi}), \quad (10)$$

$$(b) \quad \sqrt{\theta_j} | \check{\xi}_j^2, c^{\xi}, \kappa_B^2 \sim t_{2c^{\xi}} \left(0, \frac{2}{a^{\xi} \kappa_B^2} \check{\xi}_j^2 \right), \quad \check{\xi}_j^2 | a^{\xi} \sim \mathcal{G}(a^{\xi}, 1). \quad (11)$$

Additional representations for $0 < a^{\xi} < \infty$ and $0 < c^{\xi} < \infty$ based on $\phi^{\xi} = \frac{2c^{\xi}}{\kappa_B^2 a^{\xi}}$ are

$$(c) \quad \sqrt{\theta_j} | \check{\xi}_j^2, \check{\kappa}_j^2, \phi^{\xi} \sim \mathcal{N} \left(0, \phi^{\xi} \check{\xi}_j^2 / \check{\kappa}_j^2 \right), \quad \check{\xi}_j^2 | a^{\xi} \sim \mathcal{G}(a^{\xi}, 1), \quad \check{\kappa}_j^2 | c^{\xi} \sim \mathcal{G}(c^{\xi}, 1), \quad (12)$$

$$(d) \quad \sqrt{\theta_j} | \tilde{\psi}_j^2, \phi^{\xi} \sim \mathcal{N} \left(0, \phi^{\xi} \tilde{\psi}_j^2 \right), \quad \tilde{\psi}_j^2 | a^{\xi}, c^{\xi} \sim \mathcal{BP}(a^{\xi}, c^{\xi}), \quad (13)$$

where $\mathcal{BP}(a^{\xi}, c^{\xi})$ is the beta-prime distribution.¹

¹ Note that the $X \sim \mathcal{BP}(a, b)$ -distribution has pdf

$$p(x) = \frac{1}{B(a, b)} \frac{x^{a-1}}{(1+x)^{a+b}}.$$

Prior for $\sqrt{\theta_j}$		a^{ξ}	c^{ξ}	κ_B^2	ϕ^{ξ}
$\mathcal{N}\left(0, \psi_j^2\right), \psi_j^2 \sim \text{GG}\left(a^{\xi}, c^{\xi}, \phi^{\xi}\right)$	normal-gamma-gamma	a^{ξ}	c^{ξ}	$\frac{2c^{\xi}}{\phi^{\xi} a^{\xi}}$	ϕ^{ξ}
$\mathcal{N}\left(0, \frac{1}{\kappa_j} - 1\right), \kappa_j \sim \text{TPB}\left(a^{\xi}, c^{\xi}, \phi^{\xi}\right)$	generalized beta mixture	a^{ξ}	c^{ξ}	$\frac{2c^{\xi}}{\phi^{\xi} a^{\xi}}$	ϕ^{ξ}
$\mathcal{N}\left(0, \psi_j^2\right), \psi_j^2 \sim \text{SBeta2}\left(a^{\xi}, c^{\xi}, \phi^{\xi}\right)$	hierarchical scaled beta2	a^{ξ}	c^{ξ}	$\frac{2c^{\xi}}{\phi^{\xi} a^{\xi}}$	ϕ^{ξ}
$\mathcal{DE}\left(0, \sqrt{2} \psi_j\right), \psi_j^2 \sim \mathcal{G}\left(c^{\xi}, \frac{1}{\lambda^2}\right)$	normal-exponential-gamma	1	c^{ξ}	$2\lambda^2 c^{\xi}$	$\frac{1}{\lambda^2}$
$\mathcal{N}\left(0, \tau^2 \psi_j^2\right), \psi_j \sim t_1$	Horseshoe	$\frac{1}{2}$	$\frac{1}{2}$	$\frac{2}{\tau^2}$	τ^2
$\mathcal{N}\left(0, \frac{1}{\kappa_j} - 1\right), \kappa_j \sim \mathcal{B}(1/2, 1)$	Strawderman-Berger	$\frac{1}{2}$	1	4	1
$\mathcal{N}\left(0, \tau^2 \xi_j\right), \xi_j \sim \mathcal{G}\left(a^{\xi}, a^{\xi}\right)$	double gamma	a^{ξ}	∞	$\frac{2}{\tau^2}$	-
$\mathcal{N}\left(0, \tau^2 \tilde{\xi}_j\right), \tilde{\xi}_j \sim \mathcal{E}(1)$	Lasso	1	∞	$\frac{2}{\tau^2}$	-
$t_{\nu}\left(0, \tau^2\right)$	half- t	∞	$\frac{\nu}{2}$	$\frac{2}{\tau^2}$	-
$t_1\left(0, \tau^2\right)$	half-Cauchy	∞	$\frac{1}{2}$	$\frac{2}{\tau^2}$	-
$\mathcal{N}\left(0, B_0\right)$	normal	∞	∞	$\frac{2}{B_0}$	-

Table 1. Priors on $\sqrt{\theta_j}$ which are equivalent to (top) or special cases of (bottom) the triple gamma prior.

2.3. Relation of the triple gamma to other shrinkage priors

The triple gamma prior can be related to the very active research on shrinkage priors in a Bayesian framework in various ways. On the one hand, popular priors for variance parameters introduced as robust alternatives to the inverse gamma prior are special cases of the triple gamma, see Table 1. For instance, in (8), ψ_j^2 converges a.s. to 1, as $a^{\xi} \rightarrow \infty$ and $c^{\xi} \rightarrow \infty$, and the triple gamma reduces to a normal distribution for $\sqrt{\theta_j}$, applied for univariate TVP models [34] and unobserved component state space model [14]. For $c^{\xi} \rightarrow \infty$, $F(2a^{\xi}, 2c^{\xi})$ converges to the $\mathcal{G}(a^{\xi}, a^{\xi})$ distribution and the triple gamma reduces to the Bayesian Lasso for $a^{\xi} = 1$ [15] and otherwise to the double gamma [17] applied in sparse TVP models.

Gelman [21] introduced the half- t and the half-Cauchy prior for variance parameters in hierarchical models, by assuming that $\sqrt{\theta_j}$ follows a “folded” t -distribution, i.e. a t -distribution truncated to $[0, \infty)$, see also Polson and Scott [22]. In (10), ξ_j^2 converges a.s. to 1 as $a^{\xi} \rightarrow \infty$ and the triple gamma reduces to a $t_{2c^{\xi}}$ -distribution and to the Cauchy distribution for $c^{\xi} = 1/2$, however without being “folded”, since we allow $\sqrt{\theta_j}$ to take on negative values. A half- t_{ν} with $\nu = 2c^{\xi}$ and a triple gamma with $a^{\xi} = \infty$ obviously imply the same prior for θ_j , so does the negative half matter? It matters, whenever inference is performed in a parametrization involving $\sqrt{\theta_j}$ such as the non-centered parametrization (2). Restricting the prior to the positive half will lead to automatic truncation of the full conditional posterior $p(\sqrt{\theta_j} | \tilde{\beta}_0, \dots, \tilde{\beta}_T, \mathbf{y}, \cdot)$, e.g. during MCMC sampling (see Section 4). If the positive and the negative mode of the marginal posterior $p(\sqrt{\theta_j} | \mathbf{y})$ are well-separated, then this will not matter. However, if the true value of θ_j is close to or equal to zero, then $p(\sqrt{\theta_j} | \mathbf{y})$ is concentrated at zero and truncation at 0 will introduce a bias, because the negative half is missing.

On the other hand, the triple gamma prior is related to popular shrinkage priors in regression models. It extends the generalized beta mixture prior introduced by Armagan *et al.* [18] for variable selection in regression models,

$$\beta_j | \xi_j^2 \sim \mathcal{N}\left(0, \xi_j^2\right), \quad \xi_j^2 \sim \mathcal{G}\left(a^{\xi}, \lambda_j\right), \quad \lambda_j \sim \mathcal{G}\left(c^{\xi}, \phi^{\xi}\right),$$

Furthermore, $Y = X/(1 + X)$ follows the $\mathcal{B}(a, b)$ -distribution.

to variance selection in state space and TVP models. This is evident from rewriting (5) as $\xi_j^2 \sim \mathcal{G}(a^\xi, \lambda_j)$, $\lambda_j \sim \mathcal{G}(c^\xi, \phi^\xi)$. We exploit this relationship in Section 3.1 to investigate the shrinkage profile of a triple gamma prior. Using Armagan *et al.* [18, Definition 2], the triple gamma prior can be written as

$$\sqrt{\theta_j}|\rho_j \sim \mathcal{N}(0, 1/\rho_j - 1), \quad \rho_j|a^\xi, c^\xi, \phi^\xi \sim \mathcal{TPB}(a^\xi, c^\xi, \phi^\xi), \quad (14)$$

where $\mathcal{TPB}(a^\xi, c^\xi, \phi^\xi)$ is the three-parameter beta (TPB) distribution with density:

$$p(\rho_j) = \frac{1}{B(a^\xi, c^\xi)} (\phi^\xi)^{c^\xi} \rho_j^{c^\xi-1} (1-\rho_j)^{a^\xi-1} \left(1 + (\phi^\xi - 1)\rho_j\right)^{-(a^\xi+c^\xi)}. \quad (15)$$

From (14) and (15), it becomes evident that the Strawderman-Berger prior $\sqrt{\theta_j} \sim \mathcal{N}(0, 1/\rho_j - 1)$, $\rho_j \sim \mathcal{B}(1/2, 1)$ [35,36] is that special case of the triple gamma prior where $\phi^\xi = 1$, $a^\xi = 1/2$, and $c^\xi = 1$.

The special case of a triple gamma, where $a^\xi = c^\xi = 1/2$, corresponds to a Horseshoe prior [19,20] on $\sqrt{\theta_j}$ with global shrinkage parameter $\tau^2 = 2/\kappa_B^2$, since $\psi_j^2 \sim F(1, 1)$ implies that $\psi_j \sim t_1$. The Horseshoe prior has been introduced for variable selection in regression models and has been shown to have excellent theoretical properties in this context for the ‘‘nearly black’’ case [37]. The triple gamma is a generalization of the Horseshoe prior, with a similar shrinkage profile, however with much more mass close to the corner solutions. Most importantly, as will be discussed in Section 3.1, this leads to a BMA-type behaviour of the triple gamma prior for small values of a^ξ and c^ξ .

The vast literature on shrinkage priors contains many more related priors. Rescaling $\tilde{\xi}_j^2 = 2/(\kappa_B^2)\psi_j^2$ in (8), for instance, yields a representation involving a scaled beta2 distribution,²

$$\sqrt{\theta_j}|\tilde{\xi}_j^2 \sim \mathcal{N}(0, \tilde{\xi}_j^2), \quad \tilde{\xi}_j^2|a^\xi, c^\xi, \phi^\xi \sim \text{SBeta2}(a^\xi, c^\xi, \phi^\xi), \quad (16)$$

as is easily derived from (A2). The scaled beta2 was introduced by Pérez *et al.* [23] in hierarchical models as a robust prior for scale parameters, $\sqrt{\theta_j}$, and variance parameters, θ_j , alike. Based on (16), the triple gamma can be seen as a hierarchical extension of this prior which puts a scaled beta2 distribution on the scaling parameter $\tilde{\xi}_j^2$ of a Gaussian prior for $\sqrt{\theta_j}$, see Table 1. Griffin and Brown [16] termed prior (16) gamma-gamma distribution, denoted by GG(a^ξ, c^ξ, ϕ).

For $a^\xi = 1$, the triple gamma reduces to the normal-exponential-gamma which has a representation as a scale-mixture of double exponential $\mathcal{DE}(0, \sqrt{2}\psi_j)$ -distributions, see Table 1. It has been considered for variable selection in regression models [38] and locally adaptive B-spline models [39]. The R2-D2 prior suggested by Zhang *et al.* [40] for high-dimensional regression models is another special case of the triple gamma. It reads

$$\beta_j \sim \mathcal{N}(0, \sigma^2 \phi_j \omega), \quad (\phi_1, \dots, \phi_d) \sim \mathcal{D}(a^\tau, \dots, a^\tau), \quad \omega \sim \mathcal{G}(a, \tau), \quad \tau \sim \mathcal{G}(b, 1),$$

where $a = da^\tau$ and σ^2 is the residual error variance of the regression model. As shown by Zhang *et al.* [40], this implies following prior for the coefficient of determination: $R^2 \sim \mathcal{B}(a, b)$ which motivates holding a

² The pdf of a SBeta2(a, c, ϕ)-distribution reads:

$$p(x) = \frac{1}{\phi^a B(a, c)} x^{a-1} (1+x/\phi)^{-(a+c)},$$

fixed, while a^τ decrease as d increases. Using that $\phi_j \omega \sim \mathcal{G}(a^\tau, \tau)$, we can show that the R2-D2 prior is equivalent to following hierarchical normal gamma prior applied in Bitto and Frühwirth-Schnatter [17] for TVP models:

$$\beta_j | \tau_j^2 \sim \mathcal{N}(0, \tau_j^2), \quad \tau_j^2 \sim \mathcal{G}(a^\tau, a^\tau \lambda_B^2 / 2), \quad \lambda_B^2 \sim \mathcal{G}(b, 2\sigma^2 / a^\tau).$$

The popular Dirichlet-Laplace prior, $\sqrt{\theta_j} | \psi_j \sim \mathcal{DE}(0, \psi_j)$, however, is not related to the triple gamma as the *prior scale* ψ_j rather than ψ_j^2 follows a gamma distribution, see again Table 1.

2.4. Using the triple gamma for variance selection in TVP models

A challenging question is how to choose the parameters a^ξ , c^ξ and κ_B^2 or ϕ^ξ of the triple gamma prior in the context of variance selection for TVP models. In addition, in a TVP context, the shrinkage parameters a^τ , c^τ and λ_B^2 or $\phi^\tau = 2c^\tau / (a^\tau \lambda_B^2)$ for the prior (7) of the initial values have to be selected.

In high-dimensional settings it is appealing to have a prior that addresses two major issues: first, high concentration around the origin to favor strong shrinkage of small variances toward zero; second, heavy tails to introduce robustness to large variances and to avoid over-shrinkage. For the triple gamma prior, both issues are addressed through the choice of a^ξ and c^ξ , see Theorem 2. First of all, we need values $0 < a^\xi \leq 0.5$ to induce a pole at 0. Second, values of $0 < c^\xi < 0.5$ will lead to very heavy tails. For very small values of a^ξ and c^ξ , the triple Gamma is a proper prior that behaves nearly as the improper normal-Jeffrey's prior [41], where $p(\sqrt{\theta_j}) \propto 1/\sqrt{\theta_j}$ and $p(\rho_j) \propto \rho_j^{-1}(1 - \rho_j)^{-1}$.

Ideally, we would place a hyper prior distribution on all shrinkage parameters which would allow us to learn the global and the local degree of sparsity, both for the variances and the initial values. Such a hierarchical triple gamma prior introduces dependence among the local shrinkage parameters ξ_1^2, \dots, ξ_d^2 in (5) and, consequently, among $\theta_1, \dots, \theta_d$ in the joint (marginal) prior $p(\theta_1, \dots, \theta_d)$. Introducing such dependence is desirable in that it allows to learn the degree of variance sparsity in TVP models, meaning that how much a variance is shrunken toward zero depends on how close the other variances are to zero. However, first naïve approaches with rather uninformative, independent priors on κ_B^2 , a^ξ , c^ξ and λ_B^2 , a^τ , c^τ were not met with much success and we found it necessary to carefully design appropriate hyper priors.

Hierarchical versions of the Bayesian Lasso [15] and the double gamma prior [17] in TVP models are based on the gamma prior $\kappa_B^2 \sim \mathcal{G}(d_1, d_2)$. Interestingly, this choice can be seen as a heavy-tailed extension of both priors, where each marginal density $p(\sqrt{\theta_j} | d_1, d_2)$ follows a triple gamma prior with the same parameter a^ξ (being equal to one for the Bayesian Lasso) and tail index $c^\xi = d_1$. In light of this relationship, it is not surprising that very small values of d_1 were applied in these papers to ensure heavy tails of $p(\sqrt{\theta_j} | d_1, d_2)$. Since a triple gamma prior has already heavy tails, we choose a different hyperprior in the present paper.

For the case $a^\xi = c^\xi = 1/2$, the global shrinkage parameter τ of the Horseshoe prior typically follows a Cauchy prior, $\tau \sim t_1$ [19,42], see also Bhadra *et al.* [8, Section 5]. The relationship $\phi^\xi = 2/\kappa_B^2 = \tau^2$ between the various global shrinkage parameters (see Table 1) implies in this case $\phi^\xi \sim F(1, 1)$ or, equivalently, $\kappa_B^2/2 \sim F(1, 1)$.

For a triple gamma prior with arbitrary a^ξ and c^ξ , this is a special case of the following prior:

$$\frac{\kappa_B^2}{2} \left| a^\xi, c^\xi \sim F(2a^\xi, 2c^\xi), \quad (17)$$

which will be motivated in Section 3.2. Under this prior, the triple gamma prior exhibits a BMA-like behavior with a uniform prior on an appropriately defined model size (see Theorem 3). Prior (17) is equivalent with following representations:

$$\begin{aligned}\kappa_B^2 | a^\xi &\sim \mathcal{G}(a^\xi, d_2), & d_2 | a^\xi, c^\xi &\sim \mathcal{G}\left(c^\xi, \frac{2c^\xi}{a^\xi}\right), \\ \phi^\xi | a^\xi, c^\xi &\sim \mathcal{BP}(c^\xi, a^\xi).\end{aligned}\tag{18}$$

Concerning a^ξ and c^ξ , we choose the following priors:

$$2a^\xi \sim \mathcal{B}(\alpha_{a^\xi}, \beta_{a^\xi}), \quad 2c^\xi \sim \mathcal{B}(\alpha_{c^\xi}, \beta_{c^\xi}).\tag{19}$$

Hence, we are restricting the support of a^ξ and c^ξ to $(0, 0.5)$, following the insights brought to us by Theorem 2.

We follow a similar strategy for the parameters a^τ , c^τ and $\lambda_B^2(\phi^\tau)$ of the prior (7):

$$\frac{\lambda_B^2}{2} \left| a^\tau, c^\tau \sim \mathcal{F}(2a^\tau, 2c^\tau), \quad 2a^\tau \sim \mathcal{B}(\alpha_{a^\tau}, \beta_{a^\tau}), \quad 2c^\tau \sim \mathcal{B}(\alpha_{c^\tau}, \beta_{c^\tau}),\tag{20}$$

which is equivalent with $\lambda_B^2 | a^\tau \sim \mathcal{G}(a^\tau, e_2)$, $e_2 | c^\tau \sim \mathcal{G}(c^\tau, 2c^\tau/a^\tau)$, and $\phi^\tau | a^\tau, c^\tau \sim \mathcal{BP}(c^\tau, a^\tau)$.

An interesting special case is the ‘‘symmetric’’ triple gamma, where $a^\xi = c^\xi$. Despite this constraint, the favourable shrinkage behaviour is preserved and decreasing $a^\xi = c^\xi$ toward zero simultaneously leads to a high concentration around the origin and a heavy-tailed behaviour. For a symmetric triple gamma prior, $\phi^\xi = 2/\kappa_B^2$ is independent of a^ξ and c^ξ and the two global shrinkage parameters are related through $\phi^\xi = 2/\kappa_B^2$. This induces shrinkage profiles that are symmetric around $1/2$, see Section 3.1. Interestingly, a symmetric triple gamma resolves the question whether to choose a gamma or an inverse gamma prior for a variance parameter ψ_j^2 . It implies the same symmetric beta-prime distribution on the variance, $\psi_j^2 \sim \mathcal{F}(2a^\xi, 2a^\xi) = \mathcal{BP}(a^\xi, a^\xi)$, and the information, $(\psi_j^2)^{-1} \sim \mathcal{BP}(a^\xi, a^\xi)$, and can be represented as a gamma prior with the scale arising from an inverse gamma prior or, equivalently, as an inverse gamma prior with the scale arising from a gamma prior:

$$\psi_j^2 = \frac{\check{\xi}_j^2}{\check{\kappa}_j^2} \times \frac{1}{\check{\xi}_j^2}, \quad (\psi_j^2)^{-1} = \check{\kappa}_j^2 \times \frac{1}{\check{\xi}_j^2}, \quad \check{\xi}_j^2 \sim \mathcal{G}(a^\xi, 1), \quad \check{\kappa}_j^2 \sim \mathcal{G}(a^\xi, 1).$$

3. Shrinkage profiles and BMA-like behavior

3.1. Shrinkage profiles

In the sparse normal-means problem where $\mathbf{y} | \boldsymbol{\beta} \sim \mathcal{N}_d(\boldsymbol{\beta}, \sigma^2 \mathbf{I}_d)$ and $\sigma^2 = 1$, the parameter $\rho_j = 1/(1 + \psi_j^2)$ appearing in (14) is known as shrinkage factor and plays a fundamental role for comparing different shrinkage priors, as ρ_j determines shrinkage toward 0.

Also in a variance selection context, it is evident from (14) that values of $\rho_j \approx 0$ will introduce no shrinkage on θ_j , whereas values of $\rho_j \approx 1$ will introduce strong shrinkage of θ_j toward 0. Hence, the prior $p(\rho_j)$, also called shrinkage profile, will play an instrumental role in the behaviour of different shrinkage priors. Following Carvalho *et al.* [20], shrinkage priors are often compared in terms of the prior they imply on ρ_j , i.e. how they handle shrinkage for small ‘‘observations’’ (in our case innovations) and how robust they are to large ‘‘observations’’. Note that we ideally want a shrinkage profile that has a pole in zero

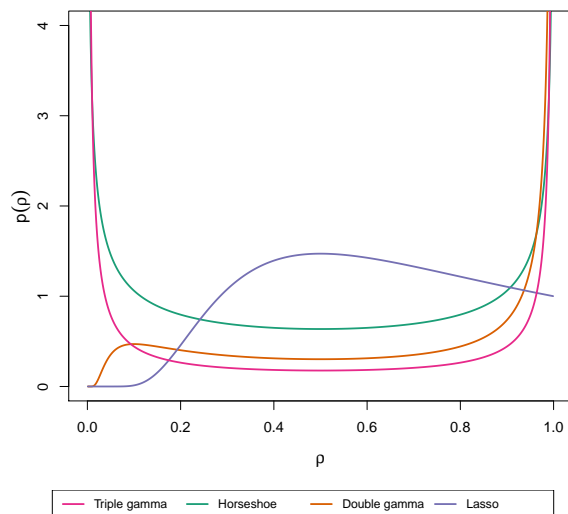


Figure 2. Marginal univariate shrinkage profile under the triple gamma prior with $a^{\xi} = c^{\xi} = 0.1$, in comparison to the Horseshoe prior, the double gamma prior with $a^{\xi} = 0.1$ the Lasso prior. $\kappa_B^2 = 2$ for all the prior specifications.

(heavy tails to avoid over-shrinking signals) and a pole in one (spikiness to shrink noise). The Horseshoe prior, e.g., implies $\rho_j \sim \mathcal{B}(1/2, 1/2)$ which is a shrinkage profile that takes this much desired form of a “Horseshoe”, see Figure 2.

For the triple gamma prior, the shrinkage profile is given by the three-parameter beta prior $p(\rho_j)$ provided in (15). For $\phi^{\xi} = 1$, $\rho_j \sim \mathcal{B}(c^{\xi}, a^{\xi})$ and $\kappa_B^2 = 2c^{\xi}/a^{\xi}$. Choosing small values $a^{\xi} \ll 1$ will put prior mass close to 1, choosing small values $c^{\xi} \ll 1$ will put prior mass close to 0, whereas values for both a^{ξ} and c^{ξ} smaller than one will induce the form of a Horseshoe prior for ρ_j . Evidently, for $\phi^{\xi} = 1$, a symmetric triple gamma prior with $a^{\xi} = c^{\xi}$ implies a Horseshoe prior for ρ_j that is symmetric around 0.5. This is illustrated in Figure 2 for a symmetric triple gamma with $a^{\xi} = c^{\xi} = 0.1$.

In Figure 2 we can also see the shrinkage profile for the Bayesian Lasso and the double gamma, which correspond to a triple gamma where $c^{\xi} \rightarrow \infty$.³ For the Bayesian Lasso with $a^{\xi} = 1$ it is clear that the shrinkage profile $p(\rho_j)$ converges to a constant for $\rho_j \rightarrow 1$, while there is no mass around $\rho_j = 0$. This means that this prior tends to over-shrink signals, while not shrinking the noise completely to zero. A double gamma prior with $a^{\xi} < 1$ has the potential to shrink the noise completely to zero, as $p(\rho_j)$ has a pole at $\rho_j = 1$, but $p(\rho_j)$ has also zero mass around $\rho_j = 0$, meaning the prior encourages over-shrinking of signals.

When we make κ_B^2 random, we obtain a “prior density” of shrinkage profiles, see Figure 3. We can see that such hierarchical versions of the Lasso and the double gamma have shrinkage profiles that resemble the ones of the Horseshoe and the triple gamma. We have used $\kappa_B^2 \sim \mathcal{G}(0.01, 0.01)$ for the Lasso and

³ Using (4), we obtain the following prior for $\rho_j = 1/(1 + \psi_j^2)$ by the law of transformation of densities:

$$p(\rho_j) = \frac{1}{\Gamma(a^{\xi})} \left(\frac{a^{\xi} \kappa_B^2}{2} \right)^{a^{\xi}} (1 - \rho_j)^{a^{\xi} - 1} \rho_j^{-(a^{\xi} + 1)} \exp \left(- \left(\frac{1 - \rho_j}{\rho_j} \right) \frac{a^{\xi} \kappa_B^2}{2} \right).$$

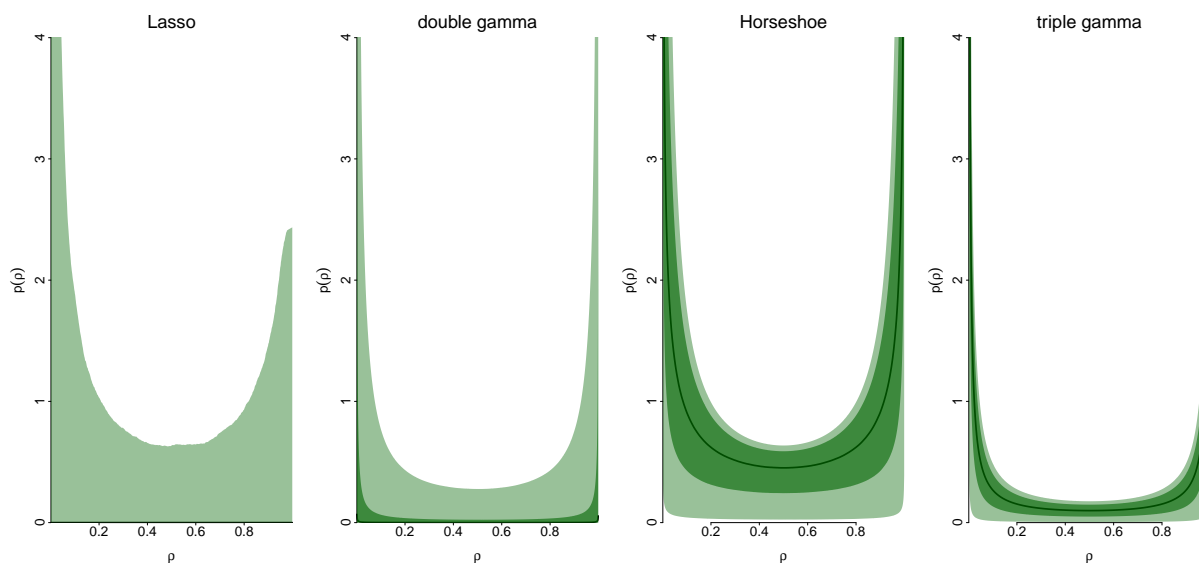


Figure 3. “Prior density” of shrinkage profiles for (from left to right) Lasso prior, double gamma prior with $a^{\xi} = 0.2$, Horseshoe prior and triple gamma prior with $a^{\xi} = c^{\xi} = 0.1$, when κ_B^2 is random. The solid line is the median, while the shaded areas represent 50% and 95 % prior credible bands. We have used $\kappa_B^2 \sim \mathcal{G}(0.01, 0.01)$ for the Lasso and the double gamma, $2/\kappa_B^2 \sim F(1, 1)$ for the Horseshoe and $2/\kappa_B^2 \sim F(0.2, 0.2)$ for the triple gamma.

the double gamma, $2/\kappa_B^2 \sim F(1, 1)$ for the Horseshoe and $2/\kappa_B^2 \sim F(0.2, 0.2)$ for the triple gamma, see Section 2.4.

3.2. BMA-type behaviour

From the perspective of Bayesian model averaging (BMA), an ideal approach for handling sparsity in TVP models would be the use of discrete mixture priors as suggested in Frühwirth-Schnatter and Wagner [14],

$$p(\sqrt{\theta_j}) = (1 - \pi)\delta_0 + \pi \cdot p_{\text{slab}}(\sqrt{\theta_j}), \quad (21)$$

with δ_0 being a Dirac measure at 0, while $p_{\text{slab}}(\sqrt{\theta_j})$ is the prior for non-zero variances. In terms of shrinkage profiles, the discrete mixture prior (21) has a spike at $\rho_j = 1$, with probability $1 - \pi$, and a lot of prior mass at $\rho_j = 0$, provided that the tails of $p_{\text{slab}}(\sqrt{\theta_j})$ are heavy enough. The mixture prior (21) is considered the “gold standard” in BMA, both theoretically and empirically, see e.g. Johnstone and Silverman [43]. However, MCMC inference under this prior is extremely challenging. As opposed to this, MCMC inference for the triple gamma prior is straightforward, see Section 4.

In this section, we relate the triple gamma prior to BMA based on the discrete mixture prior (21). An interesting insight is that the triple gamma prior shows a very similar behaviour as a discrete mixture prior, if both a^{ξ} and c^{ξ} approach zero. This induces a BMA-type behaviour on the joint shrinkage profile $p(\rho_1, \dots, \rho_d)$, with a spike at all corner solutions, where some ρ_j are very close to one, whereas the remaining ones very close to zero.

The bivariate shrinkage profiles shown in Figure 4 give us some intuition about the convergence of a symmetric triple gamma prior with $a^{\xi} = c^{\xi} \rightarrow 0$ toward a discrete spike and slab mixture. As opposed to the Lasso and the double gamma prior, the Horseshoe and the triple gamma prior put nearly all prior mass

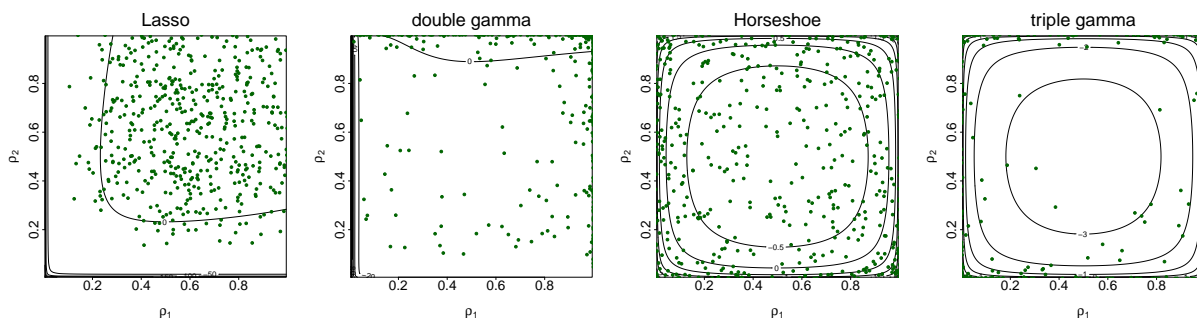


Figure 4. Bivariate shrinkage profile $p(\rho_1, \rho_2)$ for (from left to right) the Lasso prior, the double gamma prior with $a^\zeta = 0.1$, the Horseshoe prior, and the triple gamma prior with $a^\zeta = c^\zeta = 0.1$, with $\kappa_B^2 = 2$ for all the priors. The contour plots of the bivariate shrinkage profile are shown, together with 500 samples from the bivariate prior distribution of the shrinkage parameters.

on the “corner solutions”, which correspond to the four possibilities (a) $\rho_1 = \rho_2 = 0$, i.e. no shrinkage on θ_1 and θ_2 , (b) $\rho_1 = 1, \rho_2 = 0$, i.e. shrinkage of θ_1 toward 0 and no shrinkage on θ_2 , (c) $\rho_1 = 0, \rho_2 = 1$, i.e. shrinkage of θ_1 toward 0 and no shrinkage on θ_2 , and (d) $\rho_1 = \rho_2 = 1$, i.e. shrinkage of both θ_1 and θ_2 toward 0.

A very important aspect of BMA is the one of choosing a prior for the model dimension, K , see e.g. Fernández *et al.* [44] and Ley and Steel [45]. In the discrete mixture prior (21), the distribution of K depends on the choice of π . Fixing π corresponds to a very informative prior on the model dimension, for example $\pi = 0.5$ assigns more prior probability to models of dimension $d/2$ and lower prior probability to empty or full models. In fact, let δ_j be the indicator that tells us if the j -th coefficient is included in the model, then we have that $K = \sum_{j=1}^d \delta_j \sim \text{BiNom}(d, \pi)$. Placing a uniform prior for π has been shown to be a good choice, since it corresponds to placing a prior on K which is uniform on $\{0, \dots, d\}$. Note that π will be learned using information from all the variables, that it is a global parameter and will adapt to the degree of sparsity.

Following ideas in [19], we believe that a natural way to perform variable selection in the continuous shrinkage prior framework is through thresh-holding. Specifically, we say that when $(1 - \rho_j) > 0.5$, or $\rho_j < 0.5$, the variable is included, otherwise it is not. Notice that this classification via thresh-holding makes perfectly sense in the case of a triple gamma of which the Horseshoe is a special case, but less so for a Lasso or double gamma prior, even if the shrinkage profile shows a Horseshoe-like behaviour for hierarchical versions of these priors (see again Figure 3). Notice that this implies a prior on the model dimension K . Specifically,

$$K = \sum_{j=1}^d I\{\rho_j < 0.5\} \sim \text{BiNom}(d, \pi^\zeta), \quad \pi^\zeta = \Pr(\rho_j < 0.5), \quad (22)$$

where $\rho_j | a^\zeta, \phi^\zeta \sim \mathcal{TPB}(a^\zeta, b^\zeta, \phi^\zeta)$, see (15). The choice of ϕ^ζ (or κ_B^2) will strongly impact the prior on K . For a symmetric triple gamma with $a^\zeta = c^\zeta$, for instance, and fixed $\phi^\zeta = 1$, that is $\kappa_B^2 = 2$, we obtain $K \sim \text{BiNom}(d, 0.5)$, since $\pi^\zeta = 0.5$ regardless of a^ζ . Hence, we have to face similar problems as with fixing $\pi = 0.5$ for the discrete mixture prior (21).

Placing a hyper prior on ϕ^τ and ϕ^ζ or, equivalently on, λ_B^2 and κ_B^2 , as we did in Section 2.4, is as instrumental for BMA-type variable and variance selection for the triple gamma prior, as is making π

random for the discrete mixture prior (21). Ideally, we would like to have a uniform distribution on the model size K . We show in Theorem 3 that the hyperprior for κ_B^2 defined in (17) achieves exactly this goal, since π^ξ is uniformly distributed, see Appendix A for a proof.

Theorem 3. *For a hierarchical triple gamma prior with fixed $a^\xi > 0$ and $c^\xi > 0$ the probability π^ξ defined in (22) follows a uniform distribution, $\pi^\xi \sim \mathcal{U}[0, 1]$, under the hyper prior*

$$\frac{\kappa_B^2}{2} \left| a^\xi, c^\xi \sim F(2a^\xi, 2c^\xi), \quad (23)$$

or, equivalently, under the hyper prior

$$\phi^\xi | a^\xi, c^\xi \sim \mathcal{BP}(c^\xi, a^\xi). \quad (24)$$

4. MCMC algorithm

Let $\mathbf{y} = (y_1, \dots, y_T)$ be the vector of time series observations and let \mathbf{z} be the set of all latent variables and unknown model parameters in a TVP model. Moreover, let \mathbf{z}_{-x} denote the set of all unknowns but x . Bayesian inference based on MCMC sampling from the posterior $p(\mathbf{z}|\mathbf{y})$ is summarized in Algorithm 1. The hierarchical priors introduced in Section 2.4 are employed, where $(a^\tau, c^\tau, \lambda_B^2)$ follow (20), (a^ξ, c^ξ) follow (19), and κ_B^2 follows (17). For certain sampling steps, the hierarchical representation (18) is used for κ_B^2 , and similarly for λ_B^2 .

Algorithm 1 extends several existing algorithms such as the MCMC schemes introduced for the Horseshoe prior by Makalic and Schmidt [24] and for the double gamma prior by Bitto and Frühwirth-Schnatter [17]. We exploit various representations of the triple gamma prior given in Lemma 1 and choose representation (12) as the baseline representation of our MCMC algorithm:

$$\begin{aligned} \beta_j | \check{\tau}_j^2, \check{\lambda}_j^2, \phi^\tau &\sim \mathcal{N}\left(0, \phi^\tau \check{\tau}_j^2 / \check{\lambda}_j^2\right), & \check{\tau}_j^2 | a^\tau &\sim \mathcal{G}(a^\tau, 1), & \check{\lambda}_j^2 | c^\tau &\sim \mathcal{G}(c^\tau, 1), \\ \sqrt{\theta_j} | \check{\xi}_j^2, \check{\kappa}_j^2, \phi^\xi &\sim \mathcal{N}\left(0, \phi^\xi \check{\xi}_j^2 / \check{\kappa}_j^2\right), & \check{\xi}_j^2 | a^\xi &\sim \mathcal{G}(a^\xi, 1), & \check{\kappa}_j^2 | c^\xi &\sim \mathcal{G}(c^\xi, 1), \end{aligned}$$

where $\phi^\tau = 2c^\tau / (\lambda_B^2 a^\tau)$ and $\phi^\xi = 2c^\xi / (\kappa_B^2 a^\xi)$. All conditional distributions in our MCMC scheme are available in closed form, except the ones for a^ξ , c^ξ , a^τ and c^τ , for which we will resort to a MH step within Gibbs. Several conditional distributions are the same as for the double gamma prior and we apply Algorithm 1 of Bitto and Frühwirth-Schnatter [17]. We provide more details on the derivation of the various densities in Appendix B.

Algorithm 1. MCMC inference for TVP models under the triple gamma prior *Choose starting values for all global and local shrinkage parameters, i.e. $(a^\tau, c^\tau, \lambda_B^2, a^\xi, c^\xi, \kappa_B^2)$ and $\{\check{\tau}_j^2, \check{\lambda}_j^2, \check{\xi}_j^2, \check{\kappa}_j^2\}_{j=1}^d$, and repeat the following steps:*

- (a) Define for $j = 1, \dots, d$, $\tau_j^2 = \phi^\tau \check{\tau}_j^2 / \check{\lambda}_j^2$ and $\xi_j^2 = \phi^\xi \check{\xi}_j^2 / \check{\kappa}_j^2$ and sample from the posterior $p(\tilde{\beta}_0, \dots, \tilde{\beta}_T, \beta_1, \dots, \beta_d, \sqrt{\theta_1}, \dots, \sqrt{\theta_d} | \{\xi_j^2, \tau_j^2\}_{j=1}^d, \mathbf{y})$ using Algorithm 1, Steps (a), (b), and (c) in Bitto and Frühwirth-Schnatter [17]. In the homoscedastic case, use Step (f) of this algorithm to sample from $\sigma^2 | \mathbf{z}_{-\sigma^2}, \mathbf{y}$. For the SV model (3), sample the parameters μ , ϕ , and σ_η^2 as in Kastner and Frühwirth-Schnatter [46], e.g., using the R-package `stochvol` [47].
- (b) Use the prior $p(\sqrt{\theta_j} | \check{\kappa}_j^2, a^\xi, c^\xi)$, marginalized w.r.t. $\check{\xi}_j^2$, to sample a^ξ from $p(a^\xi | \mathbf{z}_{-a^\xi}, \mathbf{y})$ via a random walk MH step on $z = \log(a^\xi / (0.5 - a^\xi))$. Propose $a^{\xi,*} = 0.5e^{z^*} / (1 + e^{z^*})$, where $z^* \sim \mathcal{N}(z^{(m-1)}, v^2)$ and

$z^{(m-1)} = \log(a^{\xi, (m-1)} / (0.5 - a^{\xi, (m-1)}))$ depends on the previous value $a^{\xi, (m-1)}$ of a^ξ , accept $a^{\xi, (*)}$ with probability

$$\min \left\{ 1, \frac{q_a(a^{\xi, (*)})}{q_a(a^{\xi, (m-1)})} \right\}, \quad q_a(a^\xi) = p(a^\xi | \mathbf{z}_{-a^\xi}, \mathbf{y}) a^\xi (0.5 - a^\xi),$$

and update $\phi^\xi = 2c^\xi / (\kappa_B^2 a^\xi)$. Explicit forms for $p(a^\xi | \mathbf{z}_{-a^\xi}, \mathbf{y})$ and $\log q_a(a^\xi)$ are provided in (A3) and (A5). Similarly, use the prior $p(\beta_j | \check{\lambda}_j^2, a^\tau, c^\tau)$, marginalized w.r.t. to $\check{\tau}_j^2$, to sample a^τ via a MH step and update $\phi^\tau = 2c^\tau / (a^\tau \lambda_B^2)$.

(c) Sample $\check{\xi}_j^2$, $j = 1, \dots, d$, from a generalized inverse Gaussian distribution, see (A7):

$$\check{\xi}_j^2 | \check{\kappa}_j^2, \theta_j, a^\xi, \phi^\xi \sim \mathcal{GIG} \left(a^\xi - \frac{1}{2}, 2, \frac{\check{\kappa}_j^2 \theta_j}{\phi^\xi} \right). \quad (25)$$

Similarly, update $\check{\tau}_j^2$, $j = 1, \dots, d$, conditional on a^τ :

$$\check{\tau}_j^2 | \beta_j, \check{\lambda}_j^2, a^\tau, \phi^\tau \sim \mathcal{GIG} \left(a^\tau - \frac{1}{2}, 2, \frac{\check{\lambda}_j^2 \beta_j^2}{\phi^\tau} \right).$$

(d) Use the marginal Student-t distribution $p(\sqrt{\theta_j} | \check{\xi}_j^2, c^\xi, \kappa_B^2)$ given in (11) to sample c^ξ from $p(c^\xi | \mathbf{z}_{-c^\xi}, \mathbf{y})$ via a random walk MH step on $z = \log(c^\xi / (0.5 - c^\xi))$. Propose $c^{\xi, (*)} = 0.5e^{z^*} / (1 + e^{z^*})$, where $z^* \sim \mathcal{N}(z^{(m-1)}, v^2)$ and $z^{(m-1)} = \log(c^{\xi, (m-1)} / (0.5 - c^{\xi, (m-1)}))$ depends on the previous value $c^{\xi, (m-1)}$ of c^ξ , accept $c^{\xi, (*)}$ with probability

$$\min \left\{ 1, \frac{q_c(c^{\xi, (*)})}{q_c(c^{\xi, (m-1)})} \right\}, \quad q_c(c^\xi) = p(c^\xi | \mathbf{z}_{-c^\xi}, \mathbf{y}) c^\xi (0.5 - c^\xi),$$

and update $\phi^\xi = \frac{2c^\xi}{\kappa_B^2 a^\xi}$. Explicit forms for $p(c^\xi | \mathbf{z}_{-c^\xi}, \mathbf{y})$ and $\log q_c(c^\xi)$ are provided in (A8) and (A9).

Similarly, to sample c^τ via a MH step use the marginal distribution of $\beta_j | \check{\tau}_j^2, a^\tau, c^\tau$ with respect to $\check{\lambda}_j^2$ and update $\phi^\tau = 2c^\tau / (a^\tau \lambda_B^2)$.

(e) Sample $\check{\kappa}_j^2$, for $j = 1, \dots, d$, from following gamma distribution, see (A11):

$$\check{\kappa}_j^2 | \theta_j, \check{\xi}_j^2, c^\xi, \phi^\xi \sim \mathcal{G} \left(1/2 + c^\xi, \frac{\theta_j}{2\phi^\xi \check{\xi}_j^2} + 1 \right). \quad (26)$$

Similarly, update $\check{\lambda}_j^2$, $j = 1, \dots, d$, conditional on c^τ :

$$\check{\lambda}_j^2 | \beta_j, \check{\tau}_j^2, c^\tau, \phi^\tau \sim \mathcal{G} \left(1/2 + c^\tau, \frac{\beta_j^2}{2\phi^\tau \check{\tau}_j^2} + 1 \right).$$

(f) Sample d_2 from $d_2|a^{\xi}, c^{\xi}, \kappa_B^2 \sim \mathcal{G}\left(a^{\xi} + c^{\xi}, \kappa_B^2 + \frac{2c^{\xi}}{a^{\xi}}\right)$, see (A12); sample from κ_B^2 from following gamma distribution,

$$\kappa_B^2|\{\theta_j, \check{\kappa}_j^2, \check{\xi}_j^2\}_{j=1}^d, a^{\xi}, c^{\xi}, d_2 \sim \mathcal{G}\left(\frac{d}{2} + a^{\xi}, \frac{a^{\xi}}{4c^{\xi}} \sum_{j=1}^d \frac{\check{\kappa}_j^2}{\check{\xi}_j^2} \theta_j + d_2\right), \quad (27)$$

see (A13), and update $\phi^{\xi} = \frac{2c^{\xi}}{\kappa_B^2 a^{\xi}}$.

Similarly, sample e_2 from $e_2|a^{\tau}, c^{\tau}, \lambda_B^2 \sim \mathcal{G}\left(a^{\tau} + c^{\tau}, \lambda_B^2 + \frac{2c^{\tau}}{a^{\tau}}\right)$, sample λ_B^2 from

$$\lambda_B^2|\{\beta_j, \check{\lambda}_j^2, \check{\tau}_j^2\}_{j=1}^d, a^{\tau}, c^{\tau}, e_2 \sim \mathcal{G}\left(\frac{d}{2} + a^{\tau}, \frac{a^{\tau}}{4c^{\tau}} \sum_{j=1}^d \frac{\check{\lambda}_j^2}{\check{\tau}_j^2} \beta_j^2 + e_2\right),$$

and update $\phi^{\tau} = 2c^{\tau} / (a^{\tau} \lambda_B^2)$.

The MCMC scheme in Algorithm 1 is not a full conditional scheme, as several steps are based on partially marginalized distributions. That means that the sampling order matters. For instance, in Step (b), we marginalize w.r.t. $\check{\xi}_1^2, \dots, \check{\xi}_d^2$, hence we need to update $\check{\xi}_1^2, \dots, \check{\xi}_d^2$ after sampling a^{ξ} , before we update c^{ξ} in Step (d) conditional on $\check{\xi}_1^2, \dots, \check{\xi}_d^2$. Similarly, due to marginalization in Step (d), we need to update $\check{\kappa}_1^2, \dots, \check{\kappa}_d^2$, before we update d_2 in Step (f). Furthermore, both Step (b) and Step (d) are based on the marginal prior of κ_B^2 , given in (17). Hence, in Step (f), d_2 has to be updated from $d_2|a^{\xi}, c^{\xi}, \kappa_B^2$, before κ_B^2 is updated conditional on d_2 .

For a symmetric triple gamma prior, where $a^{\xi} = c^{\xi}$, the MCMC scheme in Algorithm 1 has to be modified only slightly. Either $q_a(a^{\xi})$ in Step (b) is adjusted and Step (d) is skipped, setting $c^{\xi} = a^{\xi}$, or $q_c(c^{\xi})$ in Step (d) is adjusted and Step (b) is skipped, setting $a^{\xi} = c^{\xi}$. In Appendix B, we provide details in (A14) for the first case and in (A15) for the second case. Similar modifications are needed, if $a^{\tau} = c^{\tau}$. All other steps in Algorithm 1 remain the same for $a^{\xi} = c^{\xi}$ and/or $a^{\tau} = c^{\tau}$.

5. Applications to TVP-VAR-SV models

5.1. Model

Consider an m -dimensional time series, $\mathbf{Y}_1, \dots, \mathbf{Y}_T$. The joint dynamics of such time series can be modeled through a time-varying parameter vector autoregressive model with stochastic volatility (TVP-VAR-SV). Since the influential paper of Primiceri [25] (see Del Negro and Primiceri [26] for a corrigendum), this model has become a benchmark for analyzing relationships between macroeconomic variables that evolve over time, see Nakajima [27], Koop and Korobilis [28], Eisenstat *et al.* [29], Chan and Eisenstat [30], Feldkircher *et al.* [31] and Carriero *et al.* [32], among many others. A TVP-VAR-SV model of order p can be expressed as follows:

$$\mathbf{Y}_t = \mathbf{c}_t + \Phi_{1,t} \mathbf{Y}_{t-1} + \Phi_{2,t} \mathbf{Y}_{t-2} + \dots + \Phi_{p,t} \mathbf{Y}_{t-p} + \boldsymbol{\varepsilon}_t, \quad \boldsymbol{\varepsilon}_t \sim \mathcal{N}_m(\mathbf{0}, \boldsymbol{\Sigma}_t), \quad (28)$$

where \mathbf{c}_t is the m -dimensional intercept, $\Phi_{j,t}$, for $j = 1, \dots, p$ is an $m \times m$ matrix of time-varying coefficients, and $\boldsymbol{\Sigma}_t$ is the time-varying variance covariance matrix of the error term. The TVP-VAR-SV model can be written in a more compact notation as

$$\mathbf{Y}_t = (\mathbb{I}_m \otimes \mathbf{X}_t) \boldsymbol{\beta}_t + \boldsymbol{\varepsilon}_t, \quad \boldsymbol{\varepsilon}_t \sim \mathcal{N}_m(\mathbf{0}, \boldsymbol{\Sigma}_t), \quad (29)$$

where $\mathbf{X}_t = (\mathbf{Y}'_{t-1}, \dots, \mathbf{Y}'_{t-p}, 1)$ is a row vector of length $mp + 1$ and $\boldsymbol{\beta}_t = (\boldsymbol{\beta}_t^1, \dots, \boldsymbol{\beta}_t^m)'$, where $\boldsymbol{\beta}_t^i = (\boldsymbol{\Phi}_{1,t,i}, \dots, \boldsymbol{\Phi}_{p,t,i}, c_{t,i})'$. Here, $\boldsymbol{\Phi}_{j,t,i}$ denotes the i -th row of the matrix $\boldsymbol{\Phi}_{j,t}$ and $c_{t,i}$ denotes the i -th element of \mathbf{c}_t .

Following Bitto and Frühwirth-Schnatter [17], we use an LDLT decomposition of the time-varying covariance matrix, that is $\boldsymbol{\Sigma}_t = \mathbf{A}_t \mathbf{D}_t \mathbf{A}_t'$, where \mathbf{D}_t is a diagonal matrix and \mathbf{A}_t is lower unitriangular matrix, see also [32]. We denote with $a_{ij,t}$ the element at the i -th row and j -th column of \mathbf{A}_t , and with $d_{i,t}$ the i -th element of the diagonal of \mathbf{D}_t . In total, we have $m(m-1)/2 + m(mp+1)$ (potentially) time-varying parameters. Using the LDLT decomposition, we can rewrite the system as:

$$\mathbf{Y}_t = (\mathbb{I}_m \otimes \mathbf{X}_t) \boldsymbol{\beta}_t + \mathbf{A}_t \boldsymbol{\eta}_t, \quad \boldsymbol{\eta}_t \sim \mathcal{N}(\mathbf{0}, \mathbf{D}_t).$$

This, in turn, allows us to write

$$\begin{aligned} y_{1,t} &= \mathbf{X}_t \boldsymbol{\beta}_t^1 + \eta_{1,t}, & \eta_{1,t} &\sim \mathcal{N}(0, d_{1,t}) \\ y_{2,t} &= \mathbf{X}_t \boldsymbol{\beta}_t^2 + a_{21,t} \eta_{1,t} + \eta_{2,t}, & \eta_{2,t} &\sim \mathcal{N}(0, d_{2,t}) \\ y_{3,t} &= \mathbf{X}_t \boldsymbol{\beta}_t^3 + a_{31,t} \eta_{1,t} + a_{32,t} \eta_{2,t} + \eta_{3,t}, & \eta_{3,t} &\sim \mathcal{N}(0, d_{3,t}) \\ & \vdots & & \end{aligned}$$

Generalizing, for the i -th equation we have that

$$y_{i,t} = \mathbf{X}_t \boldsymbol{\beta}_t^i + \sum_{j=1}^{i-1} a_{ij,t} \eta_{j,t} + \eta_{i,t}, \quad \eta_{i,t} \sim \mathcal{N}(0, d_{i,t}),$$

with independent error terms $\eta_{i,t}$ across equations. In practice, the i -th equation of the system can be written as a TVP regression model where the residuals of the preceding $i-1$ equations have been added as "regressors". The time-varying regression parameters are assumed to follow a random walk, specifically

$$\begin{aligned} \beta_{j,t}^i &= \beta_{j,t-1}^i + v_{ij,t}, & v_{ij,t} &\sim \mathcal{N}(0, \theta_{ij}^\beta), & \text{for } i = 1, \dots, m, \text{ and } j = 1, \dots, mp+1, \\ a_{ij,t} &= a_{ij,t-1} + w_{ij,t}, & w_{ij,t} &\sim \mathcal{N}(0, \theta_{ij}^a), & \text{for } i = 1, \dots, m, \text{ and } j = 1, \dots, i-1. \end{aligned}$$

with initial values $\beta_{j,0}^i \sim \mathcal{N}(\beta_{ij}^\beta, \theta_{ij}^\beta)$ and $a_{ij,0} \sim \mathcal{N}(a_{ij}^a, \theta_{ij}^a)$. Here, $\beta_{j,t}^i$ denotes the j th element of the vector $\boldsymbol{\beta}_t^i$. Shrinkage priors are then employed row wise, for the initial expectations β_{ij}^β and a_{ij}^a as well as the variances θ_{ij}^β and θ_{ij}^a . To allow for greater flexibility in the prior structure, the β_{ij}^β and a_{ij}^a are assumed to follow independent shrinkage priors, and similarly for θ_{ij}^β and θ_{ij}^a :

$$\begin{aligned} \beta_{ij}^x &\sim \mathcal{N}\left(0, \phi_i^{\tau,x} \check{\tau}_{ij}^{x,2} / \check{\lambda}_{ij}^{x,2}\right), & \check{\tau}_{ij}^{x,2} &\sim \mathcal{G}(a_i^{\tau,x}, 1), & \check{\lambda}_{ij}^{x,2} &\sim \mathcal{G}(c_i^{\tau,x}, 1), & \phi_i^{\tau,x} &= 2c_i^{\tau,x} / (\lambda_{B,i}^{x,2} a_i^{\tau,x}), \\ \sqrt{\theta_{ij}^x} &\sim \mathcal{N}\left(0, \phi_i^{\xi,x} \check{\xi}_{ij}^{x,2} / \check{\kappa}_{ij}^{x,2}\right), & \check{\xi}_{ij}^{x,2} &\sim \mathcal{G}(a_i^{\xi,x}, 1), & \check{\kappa}_{ij}^{x,2} &\sim \mathcal{G}(c_i^{\xi,x}, 1), & \phi_i^{\xi,x} &= 2c_i^{\xi,x} / (\kappa_{B,i}^{x,2} a_i^{\xi,x}), \end{aligned} \quad (30)$$

where $x = \beta$ for the VAR-coefficients and $x = a$ for the elements of \mathbf{A} . Following Section 2.4, the priors for the global shrinkage parameters read

$$\begin{aligned} \lambda_{B,i}^{x,2} | a_i^{\tau,x}, c_i^{\tau,x} &\sim \text{F}(2a_i^{\tau,x}, 2c_i^{\tau,x}), & 2a_i^{\tau,x} &\sim \mathcal{B}(\alpha_{a^\tau}, \beta_{a^\tau}), & 2c_i^{\tau,x} &\sim \mathcal{B}(\alpha_{c^\tau}, \beta_{c^\tau}), \\ \kappa_{B,i}^{x,2} | a_i^{\xi,x}, 2c_i^{\xi,x} &\sim \text{F}(2a_i^{\xi,x}, 2c_i^{\xi,x}), & 2a_i^{\xi,x} &\sim \mathcal{B}(\alpha_{a^\xi}, \beta_{a^\xi}), & 2c_i^{\xi,x} &\sim \mathcal{B}(\alpha_{c^\xi}, \beta_{c^\xi}). \end{aligned} \quad (31)$$

Finally, we assume that the idiosyncratic shocks $\eta_{i,t} \sim \mathcal{N}(0, d_{i,t})$ follow an SV model as in (3), with row specific parameters. Specifically, let $h_{i,t} = \log d_{i,t}$, we have that the logarithm of the elements of the diagonal matrix \mathbf{D} follow independent AR(1) processes:

$$h_{i,t} = \mu_i + \phi_i(h_{i,t-1} - \mu_i) + v_{i,t}, \quad v_{i,t} \sim \mathcal{N}(0, \sigma_{\eta,i}^2),$$

for $i = 1, \dots, m$. Here, μ_i is the mean of the i th log-volatility, ϕ_i is the equation specific persistence parameter, and $\sigma_{\eta,i}^2$ is the variance of the i th log-volatility.

5.2. A brief sketch of the TVP-VAR-SV MCMC algorithm

Our algorithm exploits the aforementioned unitriangular decomposition to estimate the model parameters equation-by-equation. Due to the prior structure introduced in (30), the estimation of the β_t^i and the $a_{ij,t}$ s is separated into two blocks, with the algorithm cycling through the equations, alternating between sampling β_t^i conditional on Σ_t and sampling the $a_{ij,t}$ s and $d_{i,t}$ s conditional on the VAR coefficients β_t^i . Given a set of initial values, the algorithm repeats the following steps:

Algorithm 2. MCMC inference for TVP-VAR-SV models under the triple gamma prior Choose starting values for all global and local shrinkage parameters in prior (30) for each equation and repeat the following steps:

For $i = 1, \dots, m$:

- (a) Conditional on \mathbf{A}_t and \mathbf{D}_t , create $\check{y}_{i,t} = y_{i,t} - \sum_{j=1}^{i-1} a_{ij,t}\eta_{j,t}$ and use Algorithm 1 (sans the step for the variance of the observation equation) on the TVP regression

$$\check{y}_{i,t} = \mathbf{X}_t \beta_t^i + \eta_{i,t}, \quad \eta_{i,t} \sim \mathcal{N}(0, d_{i,t}),$$

to draw from the conditional posterior distribution of the time-varying VAR-coefficients in row i , β_t^i , for $t = 0, \dots, T$, their initial expectations and process variances β_{ij}^β and θ_{ij}^β , as well as their local and global shrinkage parameters $\check{\tau}_{ij}^{\beta,2}, \check{\lambda}_{ij}^{\beta,2}, \check{\xi}_{ij}^{\beta,2}, \check{\kappa}_{ij}^{\beta,2}, \lambda_{B,i}^{\beta,2}, \kappa_{B,i}^{\beta,2}, a_i^{\tau,\beta}, c_i^{\tau,\beta}, a_i^{\xi,\beta}$, and $c_i^{\xi,\beta}$.

- (b) For $i > 1$, create $y_{i,t}^* = y_{i,t} - \mathbf{X}_t \beta_t^i$, conditional on β_t^i , and again use Algorithm 1 on the TVP regression

$$y_{i,t}^* = \sum_{j=1}^{i-1} a_{ij,t}\eta_{j,t} + \eta_{i,t}, \quad \eta_{i,t} \sim \mathcal{N}(0, d_{i,t}),$$

(where the residuals from the previous $i - 1$ equations are used as regressors) to sample the volatilities $d_{i,t}$ and the time-varying coefficients of \mathbf{A}_t in row i , $a_{ij,t}$, for $t = 0, \dots, T$ from the respective conditional posteriors, as well as the initial expectations and process variances β_{ij}^a and θ_{ij}^a and the local and global shrinkage parameters $\check{\tau}_{ij}^{a,2}, \check{\lambda}_{ij}^{a,2}, \check{\xi}_{ij}^{a,2}, \check{\kappa}_{ij}^{a,2}, \lambda_{B,i}^{a,2}, \kappa_{B,i}^{a,2}, a_i^{\tau,a}, c_i^{\tau,a}, a_i^{\xi,a}$, and $c_i^{\xi,a}$.

In the following applications, we run our algorithm for $M = 200000$ iterations, discarding the first 100000 iterations as burn-in, and then keeping the output of one every 100 iterations.

5.3. Illustrative example with simulated data

To illustrate the merit of our methodology in the context of TVP-VAR-SVs, we simulate data from two TVP-VAR-SVs with $T = 200$ points in time, $p = 1$ lags and $m = 7$ equations, with varying degrees of sparsity. In the dense regime, approximately 30% of the values of β and θ (here referring to the means of the initial states and the variances of the innovations as defined in Section 2, respectively) are truly zero,

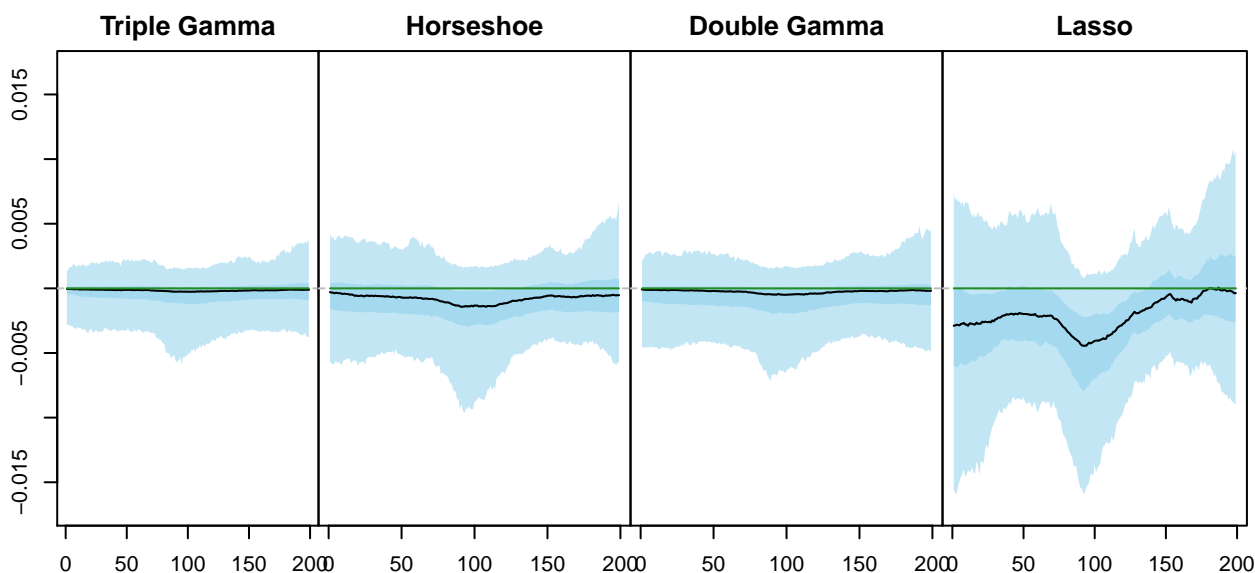


Figure 5. Posterior path against time for a constant non-significant parameter in the sparse regime.

while in the sparse regime approximately 90% are truly zero. We show results for the triple gamma prior, the Horseshoe prior, the double gamma and the Lasso.

Regarding the priors on the hyperparameters, we use prior (31) with $\alpha_{a^\tau} = \alpha_{c^\tau} = \alpha_{a^\xi} = \alpha_{c^\xi} = 1$ and $\beta_{a^\tau} = \beta_{c^\tau} = \beta_{a^\xi} = \beta_{c^\xi} = 6$ for the triple gamma. The probability density function of the corresponding beta prior is monotonically increasing, with a maximum at 0.5. This prior places positive mass in a neighborhood of the Horseshoe, but allows for more flexibility. In practice, placing a prior on the spike and slab parameters of the triple gamma, instead of fixing them to 0.5 as in the Horseshoe, allows us to learn the shrinkage profile from the data. Moreover, since the spike and the slab parameters are allowed to be different, the shrinkage profile can be asymmetric and adapt to the sparseness of the data.

We assume that the global shrinkage parameters $\lambda_{B,i}^{\beta,2}$, $\kappa_{B,i}^{\beta,2}$, $\lambda_{B,i}^{a,2}$, and $\kappa_{B,i}^{a,2}$ follow a $F(1, 1)$ distribution for the Horseshoe prior which corresponds to the prior in [19] and a $\mathcal{G}(0.001, 0.001)$ distribution for the Lasso and the double gamma prior, as suggested in [15] and [17]. Concerning the spike parameters $a_i^{\tau,a}$, $a_i^{\xi,a}$, $a_i^{\tau,\beta}$, and $a_i^{\xi,\beta}$ of the double gamma, we employ a rescaled beta prior to force them to be smaller than 0.5. Specifically, we use a $B(4, 6)$ prior which places most of its mass between 0.05 and 0.4, a range that [17] have found to induce desirable shrinkage characteristics.

Figure 5 shows the posterior path against time for a constant non-significant parameter, that is one for which $\theta_{ij}^\beta = 0$ and $\beta_{ij}^\beta = 0$ for all times, in the sparse regime. The entire set of states for the triple gamma prior can be found in Appendix C. Note that, while the zero line is contained in the 95% posterior credible interval for all priors, said interval is thinner under the triple gamma prior and the double gamma prior than under the Lasso and the Horseshoe prior. However, the light tails of the double gamma prior, as the ones of the Lasso, can over-shrink weak signals.

The above statement becomes clearer when looking at the posterior inclusion probabilities. We calculate the posterior inclusion probabilities based on the thresholding approach introduced in Section 3.2, comparing the fully unimpeded triple gamma prior to widely used special cases. Figure 6 show the posterior inclusion probability for the variance of the innovations (θ_{ij}^β 's) under four different shrinkage priors, for the sparse and the dense scenario, respectively. The cells are shaded in gray when the corresponding true state parameter is time-varying ($\theta_{ij}^\beta \neq 0$), while the background is white when

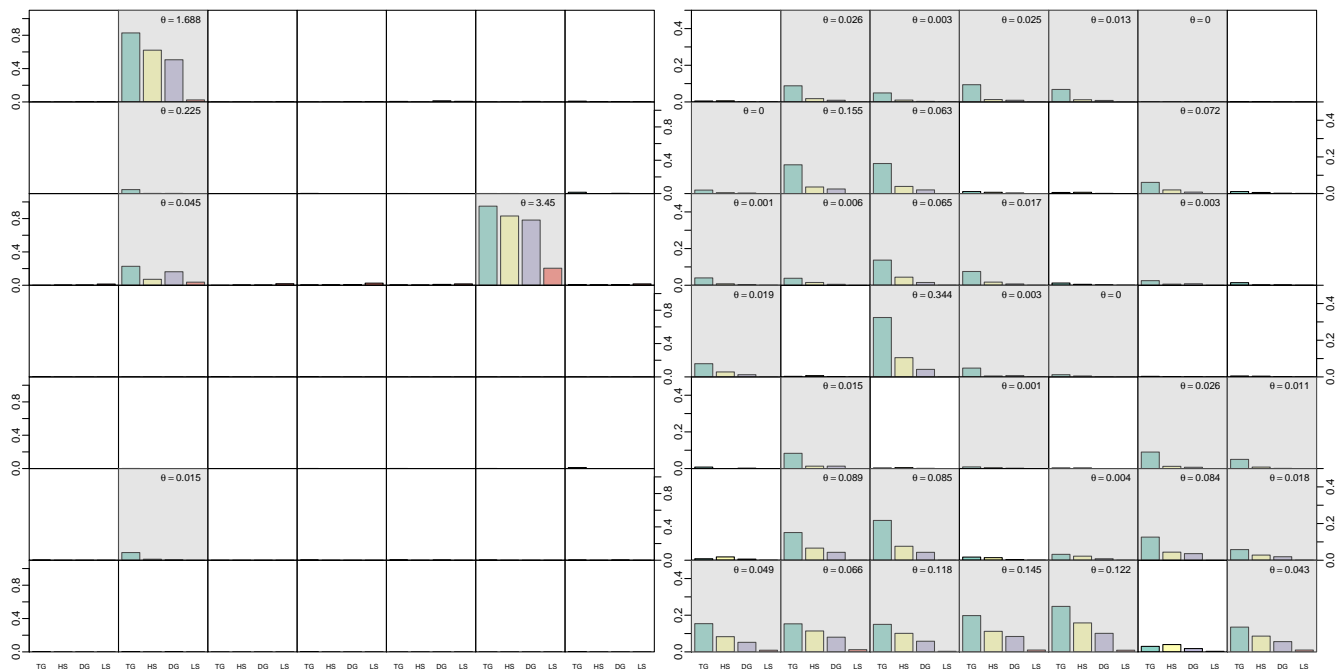


Figure 6. Posterior inclusion probability for the θ_{ij}^{β} 's in the sparse and dense regime, under the triple gamma prior, the Horseshoe prior, the Lasso prior and the double gamma prior. The true values of the θ_{ij}^{β} 's are reported in each cell.

the corresponding true state parameter is not time-varying ($\theta_{ij}^{\beta} = 0$). The posterior inclusion probabilities under the triple gamma prior are consistently higher for the states for which the parameters are actually time-varying. In some cases, that heavier tails of our prior pick up signals that the other shrinkage priors are not able to capture. On the other hand, the triple gamma identifies constant parameters, effectively pulling the appropriate θ_{ij}^{β} 's to zero.

5.4. Modeling area macroeconomic and financial variables in the Euro Area

Our application investigates a subset of the area wide model of the European Union of [48], which comprises quarterly macroeconomic data spanning from 1970 to 2017. We include 7 of the variables present in the dataset, namely real output (YER), prices (YED), short-term interest rate (STN), investment (ITR), consumption (PCR), exchange rate (EEN) and unemployment (URX). A more detailed description of the data and the transformations performed to make the time series stationary can be found in Table A2 in Appendix D. To stay in line with the literature, e.g. [49], we estimate a TVP-VAR-SV model with $p = 2$ lags on all endogenous variables. The hyperparameter choices are the same as in Section 5.3. As in the example with simulated data, we run the algorithm for $M = 200000$ iterations, discarding the first 100000 iterations as burn-in, and then keeping the output of one every 100 iterations.

Figures 7 and 8 display the posterior inclusion probabilities for the means of the initial states and the innovation variances of the VAR coefficients, respectively. A few things about Figure 7 are striking. First, the posterior inclusion probabilities on the diagonal, meaning those belonging to the parameter of each equation's own autoregressive term, appear to be those that are the highest, while off diagonal elements are more likely to be excluded. Second, the equation for the short-term interest rate is characterized by a large amount of parameters with a high inclusion probability, across all priors. Third, the first lag tends to have higher posterior inclusion probabilities than the second lag, which is in line with the literature. Finally,

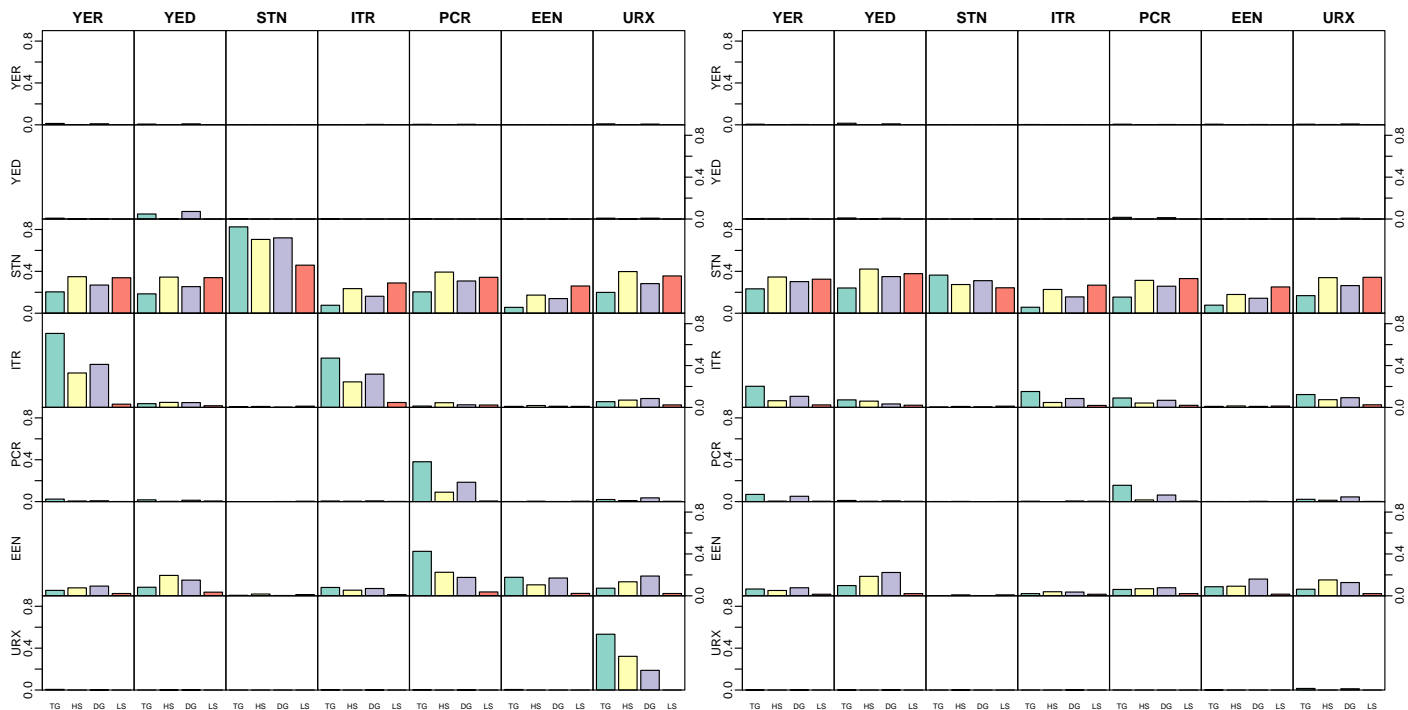


Figure 7. Posterior inclusion probability for state parameters β_{ij}^β associated with the first lag (on the left) and with the second lag (on the right), for the EA data under the triple gamma prior, the Horseshoe prior, the Lasso prior and the double gamma prior.

the triple gamma prior can be seen to often have either the largest or the smallest posterior inclusion probability compared to the other priors, which can be seen as a reflection of the high amount of prior mass placed near the shrinkage factors $\rho_{ij}^\beta = 1$ and $\rho_{ij}^\beta = 0$ of β_{ij}^β , as illustrated in Section 3. This BMA-like behavior yields a prior that is prone to be more absolute when it comes to inclusion decisions.

Now, we shift our focus to the posterior inclusion probabilities for the θ_{ij}^β 's plotted in Figure 8. Compared to the means of the initial states, almost all inclusion probabilities are essentially zero, with virtually only the triple gamma picking up (faint) signals, in particular with respect to the equations for the financial variables in the model, namely interest rate and nominal exchange rate. This lack of variability is unsurprising, as it is well known (see, e.g., [49]) that stochastic volatility in a TVP-VAR model for macroeconomic variables can explain a large part of the variability in the data. Despite this, the triple gamma, thanks to its heavy tails, is still capable of picking up weak signals in the data that the other shrinkage priors we considered are not able to discern from noise.

Given that the triple gamma tends to include more time variation than the other priors, overfitting might be considered a concern. However, Figures 9 and 10 put these fears to rest. They display the posterior median of β_{ij}^β and $|\sqrt{\theta_{ij}^\beta}|$, respectively. Here the triple gamma can be seen to be quite conservative, both in terms of which parameters to include, as well as their magnitude. In particular the medians of the $|\sqrt{\theta_{ij}^\beta}|$ are interesting, as they are closest to zero under the triple gamma prior, despite having the highest posterior inclusion probabilities among all considered priors, pointing towards the triple gamma's ability to pick up even small signals with a higher degree of confidence than other priors.

In Figures A3 and A4 in Appendix D, all the posterior paths of $\Phi_{1,t}$ and $\Phi_{2,t}$ under the triple gamma prior are shown.

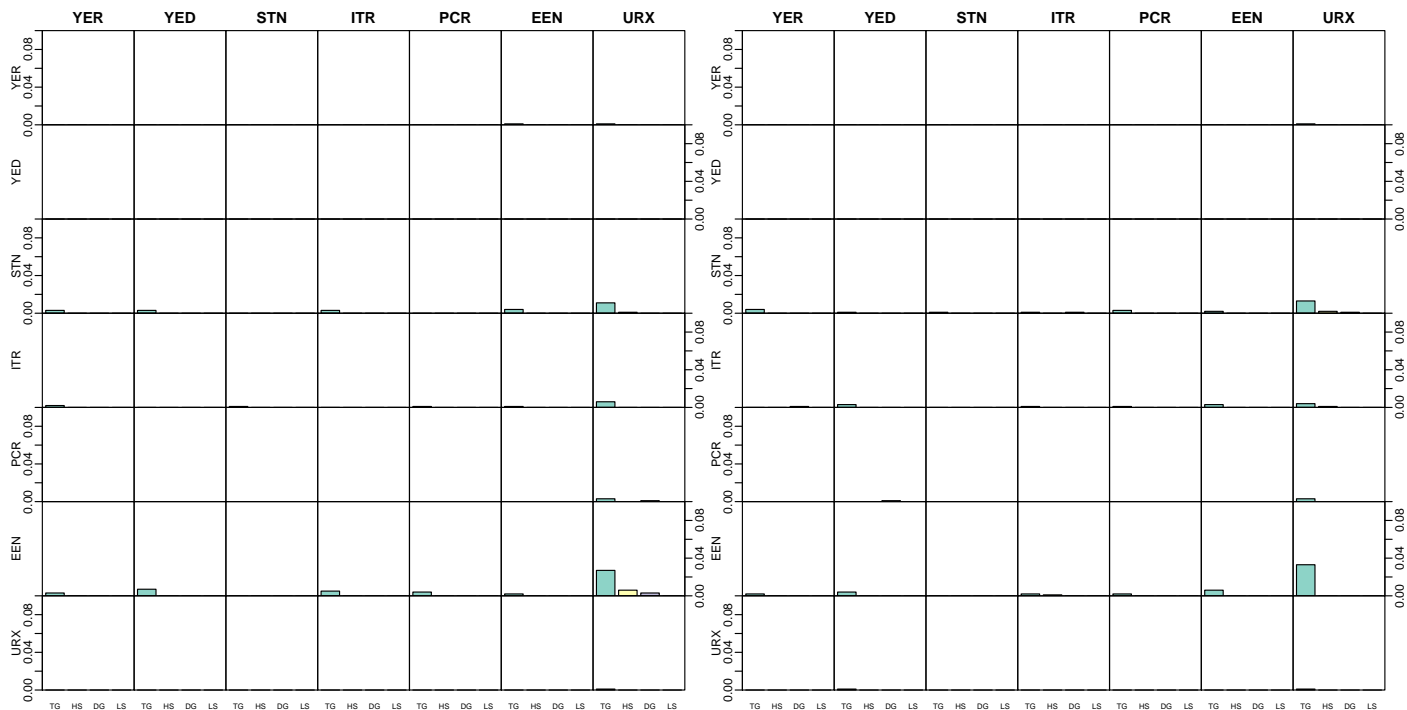


Figure 8. Posterior inclusion probability for θ_{ij}^{β} 's associated with the first lag on the left and with the second lag on the right, for the EA data under the triple gamma prior, the Horseshoe prior, the Lasso prior and the double gamma prior.

6. Conclusion

In the present paper, shrinkage for time-varying parameter (TVP) models was investigated within a Bayesian framework with the goal to automatically reduce time-varying parameters to static ones, if the model is overfitting. This goal was achieved by suggesting the triple gamma prior as a new shrinkage priors for the process variances of varying coefficients, extending previous work using spike-and-slab priors, the Bayesian Lasso, or the double gamma prior. The triple gamma prior is related to the normal-gamma-gamma prior applied for variable selection in highly structured regression models [16]. It contains the well-known Horseshoe prior as a special case, however it is more flexible, with two shape parameters that control concentration at zero and the tail behaviour. This leads to a BMA-type behaviour which allows not only variance shrinkage, but also variance selection.

In our application, we considered time-varying parameter VAR models with stochastic volatility. Overall, our findings suggest that the family of triple gamma priors introduced in this paper for sparse TVP models is successful in avoiding overfitting, if coefficients are, indeed, static or even insignificant. The framework developed in this paper is very general and holds the promise to be useful for introducing sparsity in other TVP and state space models in many different settings. Nevertheless, a number of extensions seem to be worth pursuing.

In particular, in ultra-sparse settings, modifications seem sensible. Currently, the hyperprior for the global shrinkage parameter of the triple gamma prior is selected in a way that it implies a uniform prior on “model size”. A generalization of Theorem 3 would allow to choose hyper priors that induce higher sparsity. Furthermore, in the variable selection literature, special priors such as the Horseshoe+ [50] were suggested for very sparse, ultra-high dimensional settings. Exploiting once more the non-centered

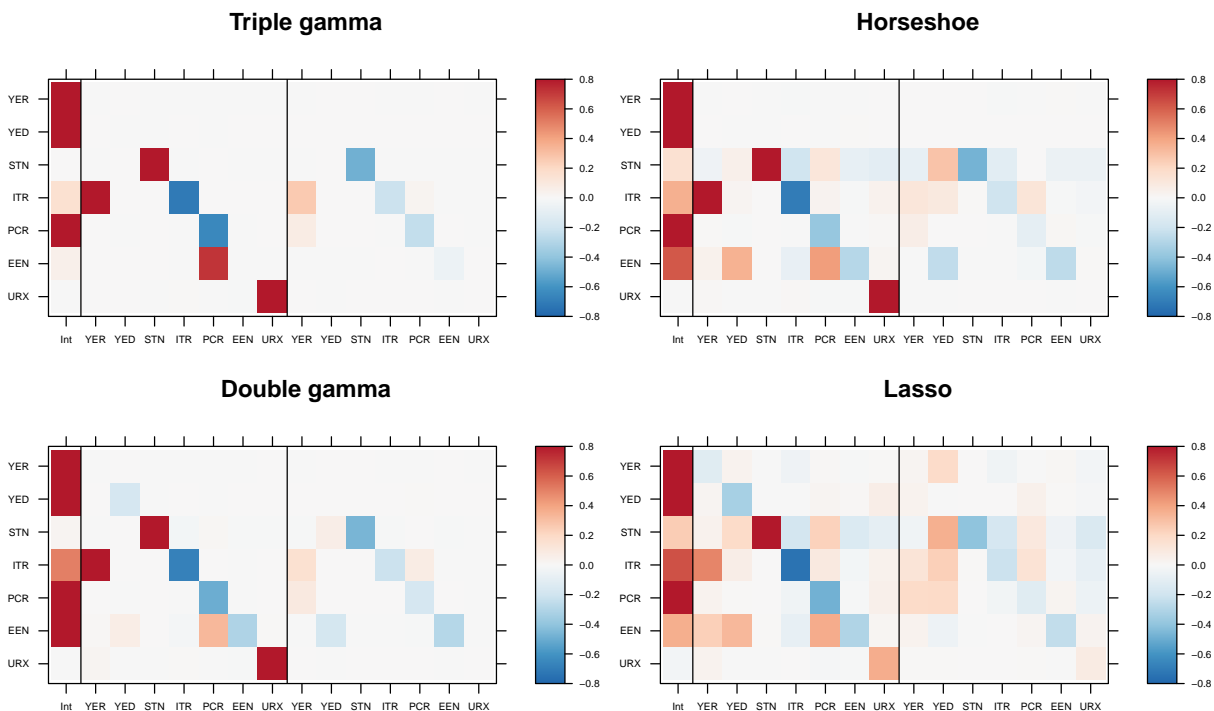


Figure 9. Posterior median of β_{ij}^{β} under the triple gamma, Horseshoe, double gamma and Lasso for the Euro area model. The vertical lines delimit the intercept, first and second lag, respectively.

parametrization of a state space model, it is straightforward to extend this prior to variance selection using following hierarchical representation:

$$\sqrt{\theta_j} \kappa_j^2, \tilde{\xi}_j^2 \sim \mathcal{N} \left(0, \frac{2}{\kappa_B^2} \kappa_j^2 \tilde{\xi}_j^2 \right), \quad \kappa_j \sim t_1, \quad \tilde{\xi}_j \sim t_1.$$

We leave both extensions for future research.

An important limitation of our approach is that shrinking a variance toward zero implies that a coefficient is fixed over the entire observation period of the time-series. In future research we will investigate dynamic shrinkage priors [51–53] where coefficients can be both fixed and dynamic.

Author Contributions: The authors contributed equally to the work.

Conflicts of Interest: The authors declare no conflict of interest.

Appendix A Proofs

Proof of Theorem 1. To proof Part (a), rewrite prior (6) in the following way by rescaling $\tilde{\xi}_j^2$ and κ_j^2 :

$$\sqrt{\theta_j} \tilde{\xi}_j^2, \tilde{\kappa}_j^2, \kappa_B^2 \sim \mathcal{N} \left(0, \frac{2}{\kappa_B^2} \frac{\tilde{\xi}_j^2}{\tilde{\kappa}_j^2} \right), \quad \tilde{\xi}_j^2 | a^{\xi} \sim \mathcal{G} \left(a^{\xi}, a^{\xi} \right), \quad \tilde{\kappa}_j^2 | c^{\xi} \sim \mathcal{G} \left(c^{\xi}, c^{\xi} \right), \quad (\text{A1})$$

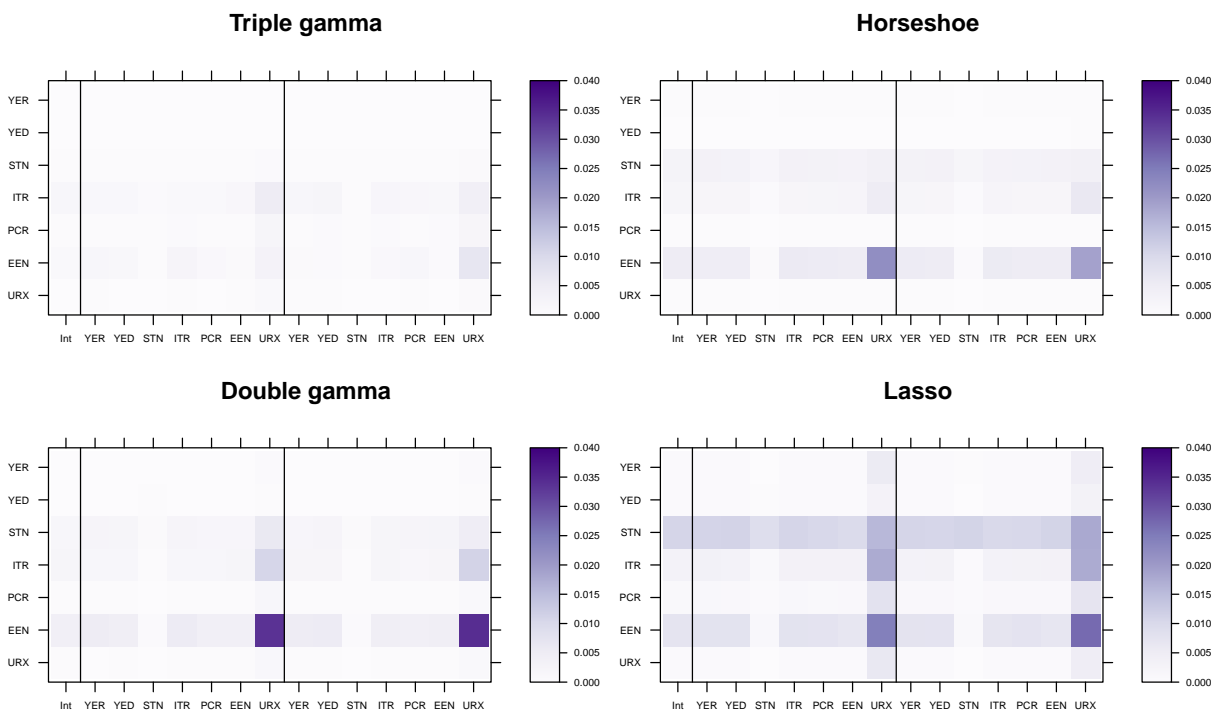


Figure 10. Posterior median of $|\sqrt{\theta_{ij}^\beta}|$ under the triple gamma, Horseshoe, double gamma and Lasso for the Euro area model. The vertical lines delimit the intercept, first and second lag, respectively

and use the fact that in (A1) the random variable $\psi_j^2 = \tilde{\xi}_j^2 / \tilde{\kappa}_j^2$ follows the F-distribution:

$$\psi_j^2 = \frac{\tilde{\xi}_j^2}{\tilde{\kappa}_j^2} \sim \frac{\mathcal{G}(a^\xi, a^\xi)}{\mathcal{G}(c^\xi, c^\xi)} =_d \text{F}(2a^\xi, 2c^\xi),$$

where $p(\psi_j^2)$ is given by:

$$p(\psi_j^2) = \frac{1}{B(a^\xi, c^\xi)} \left(\frac{a^\xi}{c^\xi} \psi_j^2 \right)^{a^\xi - 1} \left(1 + \frac{a^\xi}{c^\xi} \psi_j^2 \right)^{-(a^\xi + c^\xi)}. \quad (\text{A2})$$

This yields (8).

Using that $\eta_j = 1/\psi_j^2 \sim \text{F}(2c^\xi, 2a^\xi)$, we obtain from (8) that

$$p(\sqrt{\theta_j} | \kappa_B^2, a^\xi, c^\xi) = \frac{\sqrt{\kappa_B^2} (c^\xi)^{c^\xi}}{\sqrt{4\pi} (a^\xi)^{c^\xi} B(a^\xi, c^\xi)} \int_0^\infty \exp\left(-\frac{\theta_j \kappa_B^2 \eta_j}{4}\right) \eta_j^{c^\xi - \frac{1}{2}} \left(1 + \frac{c^\xi \eta_j}{a^\xi}\right)^{-(a^\xi + c^\xi)} \mathbf{d} \eta_j.$$

A change of variable with $y_j = c^\xi \eta_j / a^\xi$ proves Part (b):

$$\begin{aligned} p(\sqrt{\theta_j} | \phi^\xi, a^\xi, c^\xi) &= \frac{1}{\sqrt{2\pi} \phi^\xi B(a^\xi, c^\xi)} \int_0^\infty \exp\left(-\frac{\theta_j}{2\phi^\xi} y_j\right) y_j^{c^\xi - \frac{1}{2}} (1 + y_j)^{-(a^\xi + c^\xi)} \mathbf{d} y_j \\ &= \frac{\Gamma(c^\xi + \frac{1}{2})}{\sqrt{2\pi} \phi^\xi B(a^\xi, c^\xi)} U\left(c^\xi + \frac{1}{2}, \frac{3}{2} - a^\xi, \frac{\theta_j}{2\phi^\xi}\right), \end{aligned}$$

where $\phi^\xi = \frac{2c^\xi}{k_B^2 a^\xi}$. \square

Proof of Theorem 2. Using Abramowitz and Stegun [54, 13.5.8], we obtain for a and $1 < b < 2$ fixed that $U(a, b, z)$ behaves for small z as:

$$U(a, b, z) = \frac{\Gamma(b-1)}{\Gamma(a)} z^{1-b} + O(1).$$

Since $b = 3/2 - a^\xi$ in the expression for $p(\sqrt{\theta_j}|\phi^\xi, a^\xi, c^\xi)$ given in (9), the condition $1 < b < 2$ is equivalent to $0 < a^\xi < 0.5$ and this proves Part (a):

$$p(\sqrt{\theta_j}|\phi^\xi, a^\xi, c^\xi) = \frac{\Gamma(\frac{1}{2} - a^\xi)}{\sqrt{\pi}(2\phi^\xi)^{a^\xi} B(a^\xi, c^\xi)} \left(\frac{1}{\sqrt{\theta_j}} \right)^{1-2a^\xi} + O(1).$$

For $b = 1$ we obtain from Abramowitz and Stegun [54, 13.5.9] that $U(a, b, z)$ behaves for small z as follows:

$$U(a, b, z) = -\frac{1}{\Gamma(a)} (\log z + \psi(a)) + O(|z \log z|),$$

where $\psi(\cdot)$ is the digamma function. Since $b = 0$ is equivalent with $a^\xi = 0.5$, this proves Part (b):

$$p(\sqrt{\theta_j}|\phi^\xi, a^\xi, c^\xi) = \frac{1}{\sqrt{2\pi\phi^\xi} B(a^\xi, c^\xi)} \left(-\log \theta_j + \log(2\phi^\xi) - \psi(c^\xi + \frac{1}{2}) \right) + O(|\theta_j \log \theta_j|).$$

Using formulas 13.5.10-13.5.12 in Abramowitz and Stegun [54], we obtain for a and $b < 1$ fixed that $U(a, b, z)$ behaves for small z as follows:

$$U(a, b, z) = \begin{cases} \frac{\Gamma(1-b)}{\Gamma(1+a-b)} + O(z^{1-b}), & 0 < b < 1, \\ \frac{1}{\Gamma(1+a)} + O(|z \log z|), & b = 0, \\ \frac{\Gamma(1-b)}{\Gamma(1+a-b)} + O(|z|), & b < 0. \end{cases}$$

Since $O(z^{1-b})$ with $b < 1$, $O(|z \log z|)$ and $O(|z|)$ converge to 0 as $z \rightarrow 0$, we obtain:

$$\lim_{z \rightarrow 0} U(a, b, z) = \frac{\Gamma(1-b)}{\Gamma(1+a-b)}.$$

This proves Part (c) as condition $b < 1$ is equivalent to $a^\xi > 0.5$:

$$\lim_{\sqrt{\theta_j} \rightarrow 0} p(\sqrt{\theta_j}|\phi^\xi, a^\xi, c^\xi) = \frac{\Gamma(c^\xi + \frac{1}{2})}{\sqrt{2\pi\phi^\xi} B(a^\xi, c^\xi)} \lim_{z \rightarrow 0} U\left(c^\xi + \frac{1}{2}, \frac{3}{2} - a^\xi, z\right) = \frac{\Gamma(c^\xi + \frac{1}{2})\Gamma(a^\xi - \frac{1}{2})}{\sqrt{2\pi\phi^\xi} B(a^\xi, c^\xi)\Gamma(a^\xi + c^\xi)}.$$

Finally, using Abramowitz and Stegun [54, 13.1.8], we obtain as $z \rightarrow \infty$:

$$U(a, b, z) = z^{-a} \left[1 + O\left(\frac{1}{z}\right) \right], \quad b < 1.$$

Therefore as $\sqrt{\theta_j} \rightarrow \infty$

$$p(\sqrt{\theta_j}|\phi^{\bar{\zeta}}, a^{\bar{\zeta}}, c^{\bar{\zeta}}) = \frac{\Gamma(c^{\bar{\zeta}} + \frac{1}{2})(2\phi^{\bar{\zeta}})^{c^{\bar{\zeta}}}}{\sqrt{\pi}B(a^{\bar{\zeta}}, c^{\bar{\zeta}})} \left(\frac{1}{\sqrt{\theta_j}}\right)^{2c^{\bar{\zeta}}+1} \left[1 + O\left(\frac{1}{\theta_j}\right)\right].$$

□

Proof of Lemma 1. Defining $\tilde{\psi}_j^2 = \frac{a^{\bar{\zeta}}}{c^{\bar{\zeta}}} \psi_j^2$, representation (a) follows immediately from (8) and (A2). Representation (b) is obtained from (A1) by rescaling $\tilde{\zeta}_j^2$ and $\tilde{\kappa}_j^2$. To derive representation (c), integrate (A1) with respect to $\tilde{\kappa}_j^2$, using the common normal-scale mixture representation of the Student- t distribution. Finally, representation (d) is obtain from (10) by rescaling. □

Proof of Theorem 3. The equivalence of (23) and (24) follows immediately from $\phi^{\bar{\zeta}} = (c^{\bar{\zeta}}/a^{\bar{\zeta}})(2/\kappa_B^2) \sim \mathcal{BP}(c^{\bar{\zeta}}, a^{\bar{\zeta}})$, since $2/\kappa_B^2 \sim F(2c^{\bar{\zeta}}, 2a^{\bar{\zeta}})$. In addition, (24) implies that

$$\frac{\phi^{\bar{\zeta}}}{1 + \phi^{\bar{\zeta}}} \sim \mathcal{B}(c^{\bar{\zeta}}, a^{\bar{\zeta}}).$$

Using representations (13) and (14) of the tripe gamma prior, we can show:

$$\rho_j < 0.5 \Leftrightarrow \tilde{\zeta}_j^2 > 1 \Leftrightarrow \phi^{\bar{\zeta}} \tilde{\psi}_j^2 > 1 \Leftrightarrow \frac{1}{1 + \tilde{\psi}_j^2} < \frac{\phi^{\bar{\zeta}}}{1 + \phi^{\bar{\zeta}}},$$

where $\tilde{\psi}_j^2 \sim \mathcal{BP}(a^{\bar{\zeta}}, c^{\bar{\zeta}})$ and, consequently,

$$\frac{\tilde{\psi}_j^2}{1 + \tilde{\psi}_j^2} \sim \mathcal{B}(a^{\bar{\zeta}}, c^{\bar{\zeta}}) \Leftrightarrow \frac{1}{1 + \tilde{\psi}_j^2} \sim \mathcal{B}(c^{\bar{\zeta}}, a^{\bar{\zeta}}).$$

Hence, $\pi^{\bar{\zeta}} = \Pr(\rho_j < 0.5) = F_X(Y)$, where F_X is the cdf of a random variable $X \sim \mathcal{B}(c^{\bar{\zeta}}, a^{\bar{\zeta}})$ and the random variable $Y \sim \mathcal{B}(c^{\bar{\zeta}}, a^{\bar{\zeta}})$ arises from the same distribution. It follows immediately that $\pi^{\bar{\zeta}} \sim \mathcal{U}[0, 1]$. □

Appendix B Details on the MCMC scheme

In Step (b),

$$p(a^{\bar{\zeta}}|\mathbf{z}_{-a^{\bar{\zeta}}}, \mathbf{y}) \propto \left(\prod_{j=1}^d p(\sqrt{\theta_j}|\tilde{\kappa}_j^2, \phi^{\bar{\zeta}})\right) p(\kappa_B^2|a^{\bar{\zeta}}, c^{\bar{\zeta}}) p(a^{\bar{\zeta}}),$$

where $p(\kappa_B^2|a^{\bar{\zeta}}, c^{\bar{\zeta}})$ is given by:

$$p(\kappa_B^2|a^{\bar{\zeta}}, c^{\bar{\zeta}}) = \frac{1}{2^{a^{\bar{\zeta}}} B(a^{\bar{\zeta}}, c^{\bar{\zeta}})} \left(\frac{a^{\bar{\zeta}}}{c^{\bar{\zeta}}} \kappa_B^2\right)^{a^{\bar{\zeta}}-1} \left(1 + \frac{a^{\bar{\zeta}}}{2c^{\bar{\zeta}}} \kappa_B^2\right)^{-(a^{\bar{\zeta}}+c^{\bar{\zeta}})}.$$

Therefore,

$$p(a^{\zeta} | \mathbf{z}_{-a^{\zeta}}, \mathbf{y}) \propto \frac{2^{-da^{\zeta}}}{\Gamma(a^{\zeta})^d} (a^{\zeta})^{d(a^{\zeta}+1/2)/2} \left(\frac{\kappa_B^2}{c^{\zeta}} \right)^{da^{\zeta}/2} \quad (\text{A3})$$

$$\begin{aligned} & \left(\prod_{j=1}^d \check{\kappa}_j^2 \theta_j \right)^{a^{\zeta}/2} \left(\prod_{j=1}^d K_{a^{\zeta}-1/2} \left(\sqrt{\frac{\check{\kappa}_j^2 \kappa_B^2 a^{\zeta}}{c^{\zeta}}} |\sqrt{\theta_j}| \right) \right) \times \\ & \frac{1}{2^{a^{\zeta}} B(a^{\zeta}, c^{\zeta})} \left(\frac{a^{\zeta}}{c^{\zeta}} \kappa_B^2 \right)^{a^{\zeta}-1} \left(1 + \frac{a^{\zeta}}{2c^{\zeta}} \kappa_B^2 \right)^{-(a^{\zeta}+c^{\zeta})} (2a^{\zeta})^{\alpha_{a^{\zeta}}-1} (1-2a^{\zeta})^{\beta_{a^{\zeta}}-1} \end{aligned} \quad (\text{A4})$$

Hence, $\log q_a(a^{\zeta})$ is given by (using $\Gamma(a^{\zeta}) = \Gamma(a^{\zeta} + 1)/a^{\zeta}$):

$$\log q_a(a^{\zeta}) = a^{\zeta} \left(-d \log 2 + \frac{d}{2} \log \kappa_B^2 - \frac{d}{2} \log c^{\zeta} + \frac{1}{2} \sum_{j=1}^d \log \check{\kappa}_j^2 + \frac{1}{2} \sum_{j=1}^d \log \theta_j \right) \quad (\text{A5})$$

$$\begin{aligned} & + \frac{5}{4} d \log a^{\zeta} + d \frac{a^{\zeta}}{2} \log a^{\zeta} - d \log \Gamma(a^{\zeta} + 1) \\ & + \sum_{j=1}^d \log K_{a^{\zeta}-1/2} \left(\sqrt{\frac{\check{\kappa}_j^2 \kappa_B^2 a^{\zeta}}{c^{\zeta}}} |\sqrt{\theta_j}| \right) \quad (\text{prior on } \theta_j) \\ & - \log B(a^{\zeta}, c^{\zeta}) + a^{\zeta} \left(\log a^{\zeta} + \log \left(\frac{\kappa_B^2}{2c^{\zeta}} \right) \right) - \log a^{\zeta} - (a^{\zeta} + c^{\zeta}) \log \left(1 + \frac{a^{\zeta} \kappa_B^2}{2c^{\zeta}} \right) \quad (\text{prior on } \kappa_B^2) \\ & + (\alpha_{a^{\zeta}} - 1) \log(2a^{\zeta}) - (\beta_{a^{\zeta}} - 1) \log(1 - 2a^{\zeta}) \quad (\text{prior on } a^{\zeta}) \\ & + \log a^{\zeta} + \log(0.5 - a^{\zeta}) \quad (\text{change of variable}) \end{aligned} \quad (\text{A6})$$

In Step (c),

$$\begin{aligned} p(\check{\zeta}_j^2 | \mathbf{z}_{-\check{\zeta}_j^2}, \mathbf{y}) & \propto p(\sqrt{\theta_j} | \check{\zeta}_j^2, \check{\kappa}_j^2, \phi^{\zeta}) p(\check{\zeta}_j^2 | a^{\zeta}) \\ & \propto (\check{\zeta}_j^2)^{-1/2} \exp \left\{ -\frac{\check{\kappa}_j^2}{2\phi^{\zeta} \check{\zeta}_j^2} \theta_j \right\} \times (\check{\zeta}_j^2)^{a^{\zeta}-1} \exp \left\{ -\frac{\check{\zeta}_j^2}{\zeta_j} \right\} \\ & = (\check{\zeta}_j^2)^{a^{\zeta}-1/2-1} \exp \left\{ -\frac{1}{2} \left(\frac{\check{\kappa}_j^2 \theta_j}{\phi^{\zeta} \check{\zeta}_j^2} + 2\check{\zeta}_j^2 \right) \right\}, \end{aligned} \quad (\text{A7})$$

which is equal to the GIG-distribution given in (25).⁴

⁴ The pdf of the $GIG(p, a, b)$ -distribution is given by

$$f(y) = \frac{(a/b)^{p/2}}{2K_p(\sqrt{ab})} y^{p-1} e^{-\frac{1}{2}(ay+b/y)},$$

where $K_p(z)$ is the modified Bessel function.

In Step (d),

$$\begin{aligned}
p(c^{\zeta} | \mathbf{z}_{-c^{\zeta}}, \mathbf{y}) &\propto \left(\prod_{j=1}^d p(\sqrt{\theta_j} | \check{\zeta}_j^2, c^{\zeta}, \kappa_B^2) \right) p(\kappa_B^2 | a^{\zeta}, c^{\zeta}) p(c^{\zeta}) \\
&\propto \left(\prod_{j=1}^d \frac{\Gamma(\frac{2c^{\zeta}+1}{2})}{\Gamma(\frac{2c^{\zeta}}{2})} \left(2c^{\zeta} \pi \frac{2\check{\zeta}_j^2}{\kappa_B^2 a^{\zeta}} \right)^{1/2} \left(1 + \frac{1}{2c^{\zeta}} \frac{\theta_j}{\left(\frac{2\check{\zeta}_j^2}{\kappa_B^2 a^{\zeta}} \right)} \right)^{-\frac{2c^{\zeta}+1}{2}} \right) \times \\
&\quad \frac{1}{2a^{\zeta} B(a^{\zeta}, c^{\zeta})} \left(\frac{a^{\zeta}}{c^{\zeta}} \kappa_B^2 \right)^{a^{\zeta}-1} \left(1 + \frac{a^{\zeta}}{2c^{\zeta}} \kappa_B^2 \right)^{-(a^{\zeta}+c^{\zeta})} (2c^{\zeta})^{\alpha_{c^{\zeta}}-1} (1-2c^{\zeta})^{\beta_{c^{\zeta}}-1}
\end{aligned} \tag{A8}$$

Hence, $\log q_c(c^{\zeta})$ is given by (using $\Gamma(c^{\zeta}) = \Gamma(c^{\zeta} + 1)/c^{\zeta}$):

$$\begin{aligned}
\log q_c(c^{\zeta}) &= d \log \Gamma(c^{\zeta} + 0.5) - d \log \Gamma(c^{\zeta} + 1) + \frac{d}{2} \log c^{\zeta} \\
&\quad - (c^{\zeta} + 0.5) \left(\sum_{j=1}^d \log(4c^{\zeta} \check{\zeta}_j^2 + \theta_j \kappa_B^2 a^{\zeta}) - \sum_{j=1}^d \log(4c^{\zeta} \check{\zeta}_j^2) \right) \quad (\text{prior on } \theta_j) \\
&\quad - \log B(a^{\zeta}, c^{\zeta}) - (a^{\zeta} - 1) \log c^{\zeta} - (a^{\zeta} + c^{\zeta}) \log \left(1 + \frac{a^{\zeta} \kappa_B^2}{2c^{\zeta}} \right) \quad (\text{prior on } \kappa_B^2) \\
&\quad + (\alpha_{c^{\zeta}} - 1) \log(2c^{\zeta}) + (\beta_{c^{\zeta}} - 1)(1 - 2c^{\zeta}) \quad (\text{prior on } c^{\zeta}) \\
&\quad + \log c^{\zeta} + \log(0.5 - c^{\zeta}) \quad (\text{change of variable})
\end{aligned} \tag{A9}$$

In Step (e),

$$\begin{aligned}
p(\check{\kappa}_j^2 | \mathbf{z}_{-\check{\kappa}_j^2}, \mathbf{y}) &\propto p(\sqrt{\theta_j} | \check{\zeta}_j^2, \check{\kappa}_j^2, \phi^{\zeta}) p(\check{\kappa}_j^2 | c^{\zeta}) \\
&\propto (\check{\kappa}_j^2)^{1/2} \exp \left\{ -\frac{\check{\kappa}_j^2}{2\phi^{\zeta} \check{\zeta}_j^2} \theta_j \right\} \times (\check{\kappa}_j^2)^{c^{\zeta}-1} \exp \left\{ -\check{\kappa}_j^2 \right\} \\
&= (\check{\kappa}_j^2)^{1/2+c^{\zeta}-1} \exp \left\{ -\check{\kappa}_j^2 \left(\frac{\theta_j}{2\phi^{\zeta} \check{\zeta}_j^2} + 1 \right) \right\},
\end{aligned} \tag{A11}$$

which is equal to the gamma distribution given in (26).

In Step (f), $p(d_2 | \mathbf{z}_{-d_2}, \mathbf{y})$ is equal to following gamma distribution:

$$\begin{aligned}
p(d_2 | \mathbf{z}_{-d_2}, \mathbf{y}) &\propto p(\kappa_B^2 | d_2) p(d_2 | a^{\zeta}, c^{\zeta}) \\
&\propto (d_2)^{a^{\zeta}} \exp \left\{ -d_2 \kappa_B^2 \right\} (d_2)^{c^{\zeta}-1} \exp \left\{ -d_2 \frac{2c^{\zeta}}{a^{\zeta}} \right\} \\
&= (d_2)^{a^{\zeta}+c^{\zeta}-1} \exp \left\{ -d_2 \left(\kappa_B^2 + \frac{2c^{\zeta}}{a^{\zeta}} \right) \right\},
\end{aligned} \tag{A12}$$

and

$$\begin{aligned}
p(\kappa_B^2 | \mathbf{z}_{-\kappa_B^2}, \mathbf{y}) &\propto \prod_{j=1}^d p(\sqrt{\theta_j} | \xi_j^2, \check{\kappa}_j^2, \phi^\xi) p(\kappa_B^2 | d_2) \\
&\propto (\kappa_B^2)^{d/2} \exp \left\{ -\frac{\kappa_B^2 a^\xi}{4c^\xi} \sum_{j=1}^d \frac{\check{\kappa}_j^2}{\xi_j^2} \theta_j \right\} \times (\kappa_B^2)^{a^\xi-1} \exp \left\{ -d_2 \kappa_B^2 \right\} \\
&= (\kappa_B^2)^{d/2+a^\xi-1} \exp \left\{ -\kappa_B^2 \left(\frac{a^\xi}{4c^\xi} \sum_{j=1}^d \frac{\check{\kappa}_j^2}{\xi_j^2} \theta_j + d_2 \right) \right\}
\end{aligned} \tag{A13}$$

which is equal to the gamma distribution given in (27).

For a symmetric triple gamma prior, where $a^\xi = c^\xi$, Step (b) is modified in the following way, if Step (d) is dropped:

$$q_a(a^\xi) = p(a^\xi | \mathbf{z}_{-a^\xi}, \mathbf{y}) \prod_{j=1}^d p(\check{\kappa}_j^2 | c^\xi = a^\xi) \propto p(a^\xi | \mathbf{z}_{-a^\xi}, \mathbf{y}) \frac{1}{\Gamma(a^\xi)^d} \left(\prod_{j=1}^d \check{\kappa}_j^2 \right)^{a^\xi}, \tag{A14}$$

where $p(a^\xi | \mathbf{z}_{-a^\xi}, \mathbf{y})$ is given by (A3). If Step (b) is dropped, then Step (d) is modified in the following way:

$$q_c(c^\xi) = p(c^\xi | \mathbf{z}_{-c^\xi}, \mathbf{y}) \prod_{j=1}^d p(\xi_j^2 | a^\xi = c^\xi) \propto p(c^\xi | \mathbf{z}_{-c^\xi}, \mathbf{y}) \frac{1}{\Gamma(c^\xi)^d} \left(\prod_{j=1}^d \xi_j^2 \right)^{c^\xi}, \tag{A15}$$

where $p(c^\xi | \mathbf{z}_{-c^\xi}, \mathbf{y})$ is given by (A8).

Appendix C Posterior paths for the simulated data

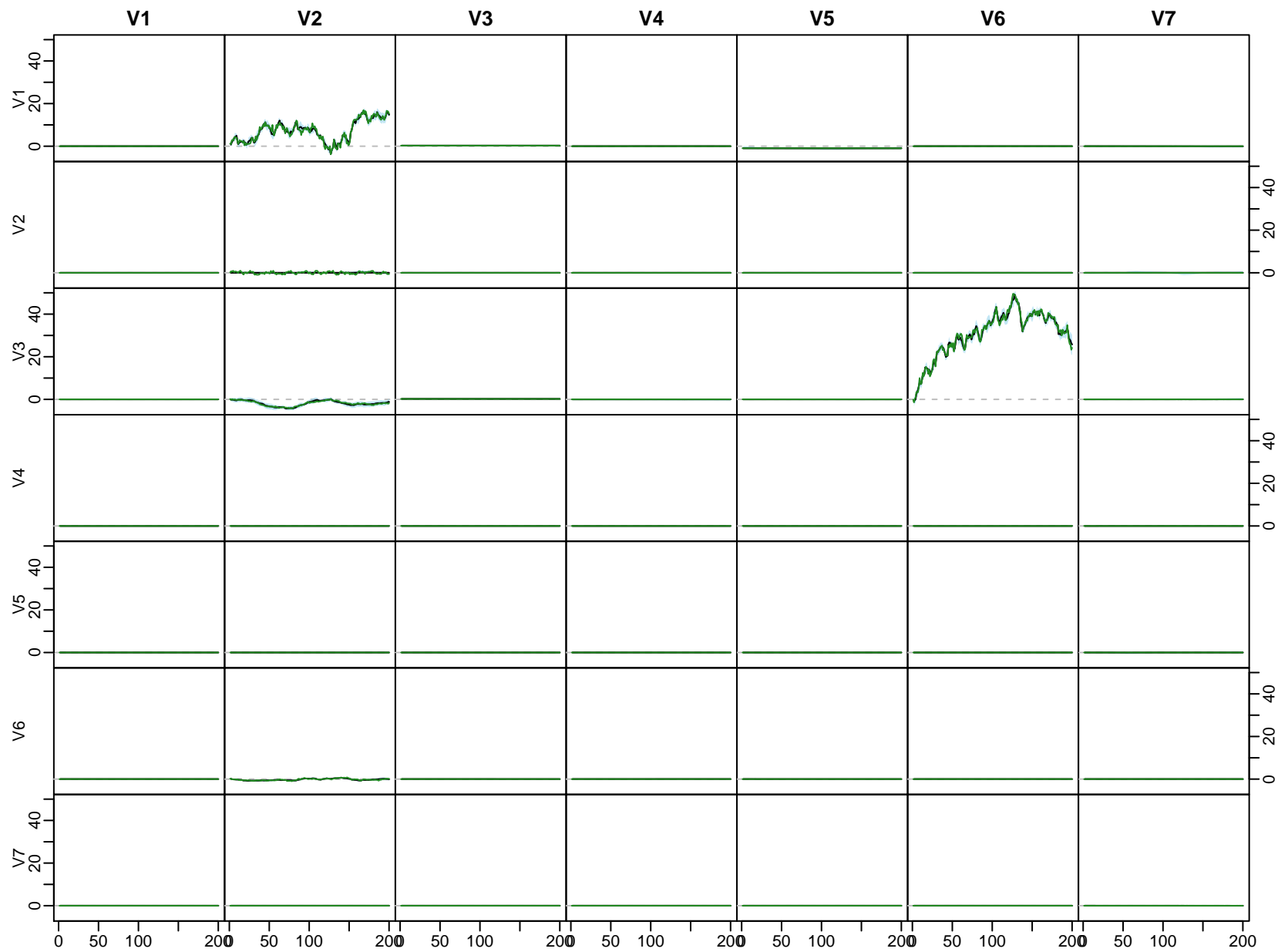


Figure A1. Each cell represents the corresponding state of the matrix $\Phi_{1,t}$, for $t = 1, \dots, T$, for the sparse regime described in Section 5.3. The solid line is the median and the shaded areas represent 50% and 95% posterior credible intervals.

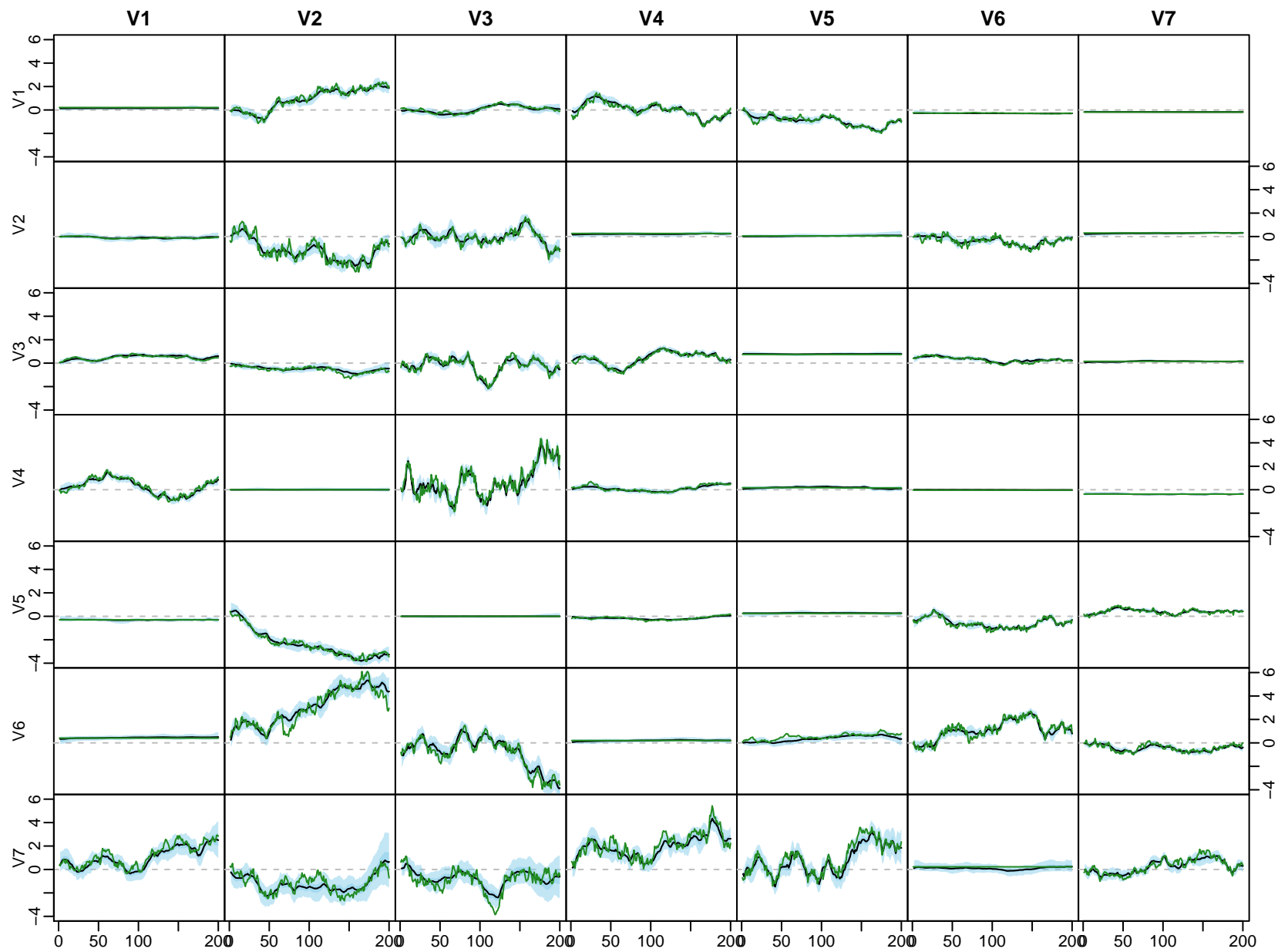


Figure A2. Each cell represents the corresponding state of the matrix $\Phi_{1,t}$, for $t = 1, \dots, T$, for the dense regime described in Section 5.3. The solid line is the median and the shaded areas represent 50% and 95% posterior credible intervals.

Appendix D Application

Appendix D.1 Data overview

Variable	Abbreviation	Description	Tcode
Real output	YER	Gross domestic product (GDP) at market prices in millions of Euros, chain linked volume, calendar and seasonally adjusted data, reference year 1995.	1
Prices	YED	GDP deflator, index base year 1995. Defined as the ratio of nominal and real GDP.	1
Short-term interest rate	STN	Nominal short-term interest rate, Euribor 3-month, percent per annum	2
Investment	ITR	Gross fixed capital formation in millions of Euros, chain linked volume, calendar and seasonally adjusted data, reference year 1995.	1
Consumption	PCR	Individual consumption expenditure in millions of Euros, chain linked volume, calendar and seasonally adjusted data, reference year 1995.	1
Exchange rate	EEN	Nominal effective exchange rate, Euro area-19 countries vis-à-vis the NEER-38 group of main trading partners, index base Q1 1999.	1
Unemployment	URX	Unemployment rate, percentage of civilian work force, total across age and sex, seasonally adjusted, but not working day adjusted.	2

Note: Data was retrieved from <https://eabcn.org/page/area-wide-model>. Tcode = 1 indicates that differences of logs were taken, while Tcode = 2 implies that the raw data was used.

Table A2. Data overview

Appendix D.2 Posterior paths

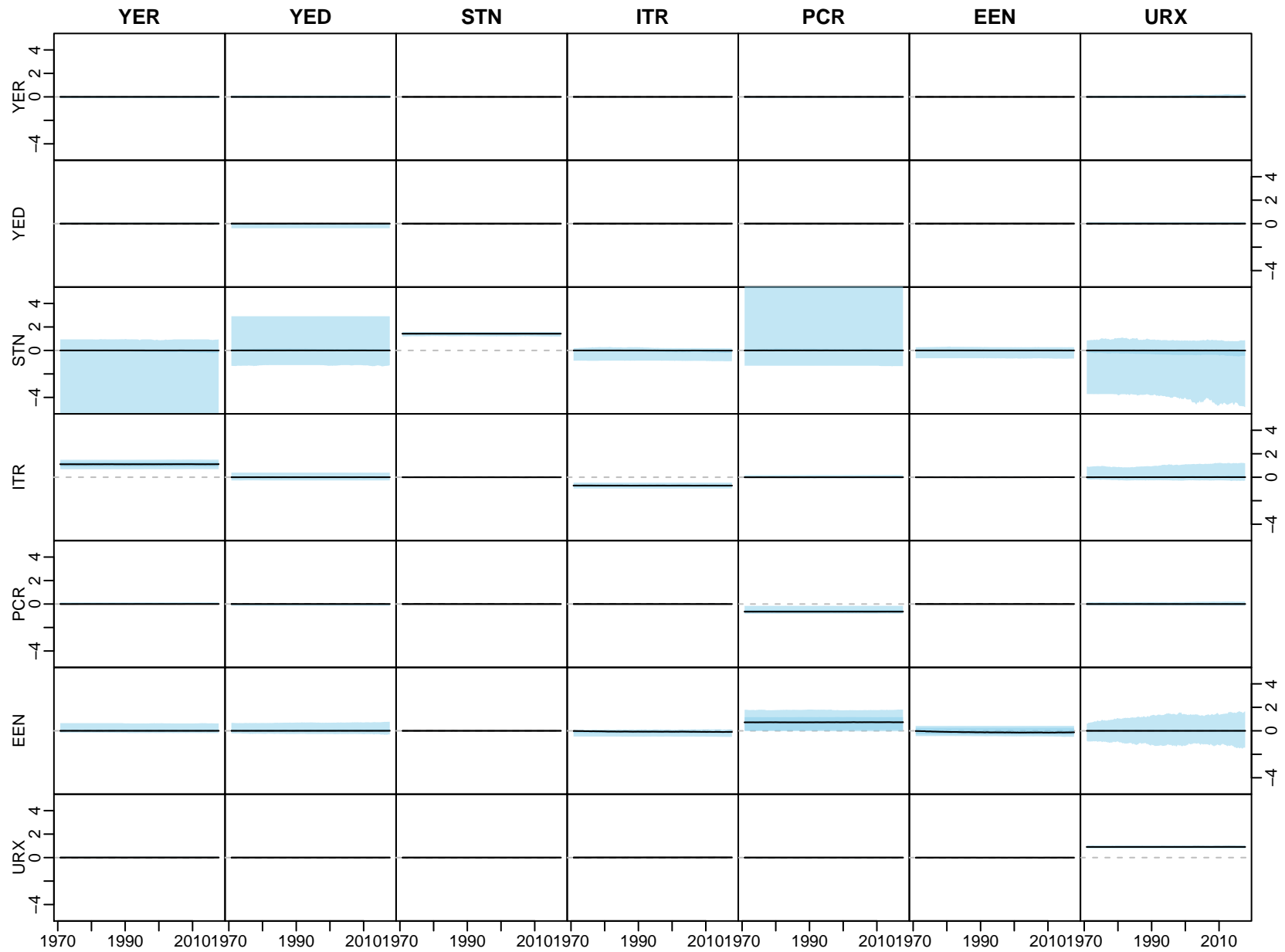


Figure A3. Each cell represents the corresponding state of the matrix $\Phi_{1,t}$, for $t = 1, \dots, T$, for the data described in Section 5.4. The solid line is the median and the shaded areas represent 50% and 95% posterior credible intervals.

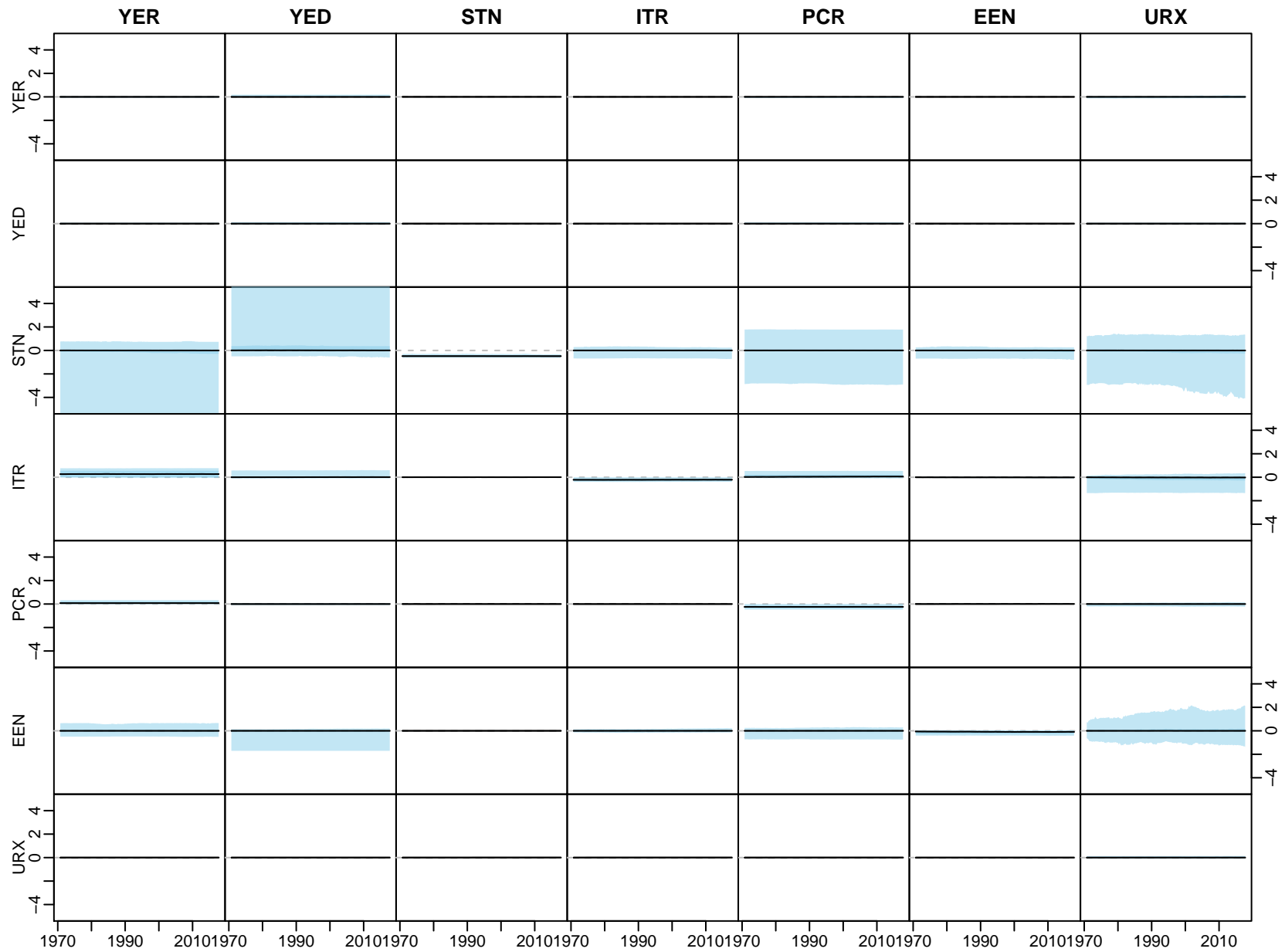


Figure A4. Each cell represents the corresponding state of the matrix $\Phi_{2,t}$, for $t = 1, \dots, T$, for the data described in section 5.4. The solid line is the median and the shaded areas represent 50% and 95% posterior credible intervals.

References

1. Raftery, A.E.; Madigan, D.; Hoeting, J. Bayesian model averaging for linear regression models. *Journal of the American Statistical Association* **1997**, *92*, 179–191. CHECK.
2. Brown, P.J.; Vannucci, M.; Fearn, T. Bayes model averaging with selection of regressors. *Journal of the Royal Statistical Society, Ser. B* **2002**, *64*, 519–536.
3. Cottet, R.; Kohn, R.J.; Nott, D.J. Variable selection and model averaging in semiparametric overdispersed generalized linear models. *Journal of the American Statistical Association* **2008**, *103*, 661–671.
4. Koop, G.; Potter, S.M. Forecasting in dynamic factor models using Bayesian model averaging. *Econometrics Journal* **2004**, *7*, 550–565.
5. Sala-i-Martin, X.X.; Doppelhofer, G.; Miller, R.I. Determinants of long-term growth: A Bayesian averaging of classical estimates (BACE) approach. *The American Economic Review* **2004**, *94*, 813–835.
6. Kleijn, R.; van Dijk, H.K. Bayes model averaging of cyclical decompositions in economic time series. *Journal of Applied Econometrics* **2006**, *21*, 191–212.
7. Frühwirth-Schnatter, S.; Tüchler, R. Bayesian Parsimonious Covariance Estimation for Hierarchical Linear Mixed Models. *Statistics and Computing* **2008**, *18*, 1–13.
8. Bhadra, A.; Datta, J.; Polson, N.G.; Willard, B. Lasso meets horseshoe: A survey. [arXiv:1706.10179v4](https://arxiv.org/abs/1706.10179v4) **2019**.
9. Fahrmeir, L.; Kneib, T.; Konrath, S. Bayesian Regularisation in Structured Additive Regression: A Unifying Perspective on Shrinkage, Smoothing and Predictor Selection. *Statistics and Computing* **2010**, *20*, 203–219.
10. Polson, N.G.; Scott, J.G. Local shrinkage rules, Lévy processes, and regularized regression. *Journal of the Royal Statistical Society, Ser. B* **2012**, *74*, 287–311.
11. Tibshirani, R. Regression shrinkage and selection via the Lasso. *Journal of the Royal Statistical Society, Ser. B* **1996**, *58*, 267–288.
12. Park, T.; Casella, G. The Bayesian Lasso. *Journal of the American Statistical Association* **2008**, *103*, 681–686.
13. Polson, N.G.; Scott, J.G. Shrink Globally, Act Locally: Sparse Bayesian Regularization and Prediction. In *Bayesian Statistics 9*; Bernardo, J.M.; Bayarri, M.J.; Berger, J.O.; Dawid, A.P.; Heckerman, D.; Smith, A.F.M.; West, M., Eds.; Oxford University Press: Oxford (UK), 2011; pp. 501–538.
14. Frühwirth-Schnatter, S.; Wagner, H. Stochastic Model Specification Search for Gaussian and partially Non-Gaussian State Space Models. *Journal of Econometrics* **2010**, *154*, 85–100.
15. Belmonte, M.A.G.; Koop, G.; Korobilis, D. Hierarchical shrinkage in time-varying parameter models. *Journal of Forecasting* **2014**, *33*, 80–94.
16. Griffin, J.E.; Brown, P.J. Hierarchical Shrinkage Priors for Regression Models. *Bayesian Analysis* **2017**, *12*, 135–159.
17. Bitto, A.; Frühwirth-Schnatter, S. Achieving Shrinkage in a Time-Varying Parameter Model Framework. *Journal of Econometrics* **2019**, *210*, 75–97.
18. Armagan, A.; Dunson, D.B.; Clyde, M. Generalized beta mixtures of Gaussians. *Advances in Neural Information Processing Systems*, 2011, pp. 523–531.
19. Carvalho, C.M.; Polson, N.G.; Scott, J.G. Handling sparsity via the horseshoe. *Journal of Machine Learning Research W&CP* **2009**, *5*, 73–80.
20. Carvalho, C.M.; Polson, N.G.; Scott, J.G. The horseshoe estimator for sparse signals. *Biometrika* **2010**, *97*, 465–480.
21. Gelman, A. Prior distributions for variance parameters in hierarchical models (Comment on Article by Browne and Draper). *Bayesian Analysis* **2006**, *1*, 515–534.
22. Polson, N.G.; Scott, J.G. On the half-Cauchy prior for a global scale parameter. *Bayesian Analysis* **2012**, *7*, 887–902.
23. Pérez, M.; Pericchi, L.R.; Ramírez, I.C. The scaled beta2 distribution as a robust prior for scales. *Bayesian Analysis* **2017**, *12*, 615–637.
24. Makalic, E.; Schmidt, D.F. A simple sampler for the horseshoe estimator. *IEEE Signal Processing Letters* **2016**, *23*, 179–182.
25. Primiceri, G. Time varying structural vector autoregressions and monetary policy. *Review of Economic Studies* **2005**, *72*, 821–852.

26. Del Negro, M.; Primiceri, G.E. Time Varying Structural Vector Autoregressions and Monetary Policy: A Corrigendum. *The Review of Economic Studies* **2015**, *82*, 1342–1345.
27. Nakajima, J. Time-varying parameter VAR model with stochastic volatility: An overview of methodology and empirical applications. *Monetary and Economic Studies* **2011**, *29*, 107–142.
28. Koop, G.; Korobilis, D. Large time-varying parameter VARs. *Journal of Econometrics* **2013**, *177*, 185 – 198.
29. Eisenstat, E.; Chan, J.C.; Strachan, R.W. Stochastic Model Specification Search for Time-Varying Parameter VARs. *SSRN Electronic Journal 01/2014*; DOI: 10.2139/ssrn.2403560 **2014**.
30. Chan, J.C.; Eisenstat, E. Bayesian model comparison for time-varying parameter VARs with stochastic volatility. *Journal of Applied Econometrics* **2016**, *218*, 1–24.
31. Feldkircher, M.; Huber, F.; Kastner, G. Sophisticated and small versus simple and sizeable: When does it pay off to introduce drifting coefficients in Bayesian VARs. *arXiv: 1711.00564* **2017**, ADD, ADD.
32. Carriero, A.; Clark, T.G.; Marcellino, M. Large Bayesian vector autoregressions with stochastic volatility and non-conjugate priors. *Journal of Econometrics* **2019**, *forthcoming*, XX–XX.
33. Jacquier, E.; Polson, N.G.; Rossi, P.E. Bayesian analysis of stochastic volatility models. *Journal of Business & Economic Statistics* **1994**, *12*, 371–417.
34. Frühwirth-Schnatter, S. Efficient Bayesian Parameter Estimation. In *State Space and Unobserved Component Models: Theory and Applications*; Harvey, A.; Koopman, S.J.; Shephard, N., Eds.; Cambridge University Press: Cambridge, 2004; pp. 123–151.
35. Strawderman, W. Proper Bayes minmax estimators of the multivariate normal mean. *The Annals of Statistics* **1971**, *42*, 385–388.
36. Berger, J.O. A robust generalized Bayes estimator and confidence region for a multivariate normal mean. *The Annals of Statistics* **1980**, *8*, 716–761.
37. van der Pas, S.; Kleijn, B.; van der Vaart, A. The horseshoe estimator: Posterior concentration around nearly black vectors. *Electronic Journal of Statistics* **2014**, *8*, 2585–2618.
38. Griffin, J.E.; Brown, P.J. BAYESIAN HYPER-LASSOS WITH NON-CONVEX PENALIZATION. *Australian & New Zealand Journal of Statistics* **2011**, *53*, 423–442.
39. Scheipl, F.; Kneib, T. Locally adaptive Bayesian p-splines with a normal-exponential-gamma prior. *Computational Statistics and Data Analysis* **2009**, *53*, 3533–3552.
40. Zhang, Y.; Reich, B.J.; Bondell, H.D. High dimensional linear regression via the R2-D2 shrinkage prior. Technical report, *arXiv: 1609.00046v2*, 2017.
41. Figueiredo, M.A.T. Adaptive sparseness for supervised learning. *IEEE Transaction on Pattern Analysis and Machine Intelligence* **2003**, *25*, 1150–1159.
42. Bhadra, A.; Datta, J.; Polson, N.; Willard, B. Horseshoe regularization for feature subset selection. *arXiv: 1702.07400*, 2017.
43. Johnstone, I.M.; Silverman, B.W. Needles and straw in haystacks: empirical Bayes estimates of possibly sparse sequences. *The Annals of Statistics* **2004**, *32*, 1594–1649.
44. Fernández, C.; Ley, E.; Steel, M.F.J. Benchmark priors for Bayesian model averaging. *Journal of Econometrics* **2001**, *100*, 381–427.
45. Ley, E.; Steel, M.F.J. On the effect of prior assumptions in Bayesian model averaging with applications to growth regression. *Journal of Applied Econometrics* **2009**, *24*, 651–674.
46. Kastner, G.; Frühwirth-Schnatter, S. Ancillarity-sufficiency interweaving strategy (ASIS) for boosting MCMC estimation of stochastic volatility models. *Computational Statistics and Data Analysis* **2014**, *76*, 408–423.
47. Kastner, G. Dealing with Stochastic Volatility in Time Series Using the R Package stochvol. *Journal of Statistical Software* **2016**, *69*, 1–30.
48. Fagan, G.; Henry, J.; Mestre, R. An area-wide model for the euro area. *Economic Modelling* **2005**, *22*, 39–59.
49. Feldkircher, M.; Huber, F.; Kastner, G. Sophisticated and small versus simple and sizeable: When does it pay off to introduce drifting coefficients in Bayesian VARs?, 2017, [[arXiv:stat.ME/1711.00564](https://arxiv.org/abs/1711.00564)].
50. Bhadra, A.; Datta, J.; Polson, N.; Willard, B. The horseshoe+ estimator of ultra-sparse signals. *Bayesian Analysis* **2017**, *12*, 1105–1131.

51. Kalli, M.; Griffin, J.E. Time-varying sparsity in dynamic regression models. *Journal of Econometrics* **2014**, *178*, 779–793.
52. Kowal, D.; Matteson, D.S.; Ruppert, D. Dynamic shrinkage processes. *Journal of the Royal Statistical Society, Ser. B* **2019**.
53. Ročková, V.; McAlinn, K. Dynamic Variable Selection with Spike-and-Slab Process Priors **2019**. arXiv:1708.00085.
54. Abramowitz, M.; Stegun, I.A., Eds. *Handbook of Mathematical Functions*, New York, 1973. Dover Publications.

Sample Availability: Samples of the compounds are available from the authors.